



# Prospects of a hot spring–originated novel cyanobacterium, *Scytonema ambikapurensis*, for wastewater treatment and exopolysaccharide-enriched biomass production

Tameshwar Prasad Jaiswal<sup>1</sup> · Sindhunath Chakraborty<sup>2</sup> · Sanjay Sharma<sup>1</sup> · Aditi Mishra<sup>1</sup> · Arun Kumar Mishra<sup>2</sup> · Satya Shila Singh<sup>1</sup>

Received: 19 August 2022 / Accepted: 16 February 2023 / Published online: 1 March 2023  
© The Author(s), under exclusive licence to Springer-Verlag GmbH Germany, part of Springer Nature 2023

## Abstract

The present work performs the polyphasic characterization of a novel cyanobacterial species *Scytonema ambikapurensis* isolated from an Indian hot spring and evaluates its wastewater bioremediation potential. While the physicochemical analyses of the wastewater indicated high load of nutrients and metals, the wastewater bioremediation experiment performed using the test cyanobacterium denoted the removal of 70 and 86% phosphate, 49 and 66% sulfate, 96 and 98% nitrate, 91 and 92% nitrite, 95 and 96% ammonia, 66 and 72% chloride, 79 and 81% zinc, 68 and 80% nickel, 81 and 90% calcium, and 80 and 90% potassium from the autoclaved and un-autoclaved wastewater, respectively, after 20 days of culturing. The kinetics study of zinc and nickel removal from wastewater revealed that the cyanobacterium employed sequential biosorption (by following pseudo-second-order kinetics model) and bioaccumulation methods to remove these two metals. The quality of the autoclaved and un-autoclaved wastewater was further improved by the cyanobacterium through reduction of hardness by 74 and 81%, respectively. In wastewater, the cyanobacterium not only enhanced its biomass, chlorophyll and carbohydrate contents, but also produced small amount of released and high capsular exopolysaccharide (EPS). The FTIR and TGA analyses of capsular EPS unraveled that it was a negatively charged sulfated biomolecule having thermostability up to 240 °C, which suggested its possible use as excellent emulsifying, viscosifying, and biosorption agent. The credibility of this EPS as biosorption agent was ascertained by evaluating its metal chelating ability. Finally, the experimental data denoting the ability of *S. ambikapurensis* to bioremediate wastewater and simultaneously produce EPS was statistically validated by PCA1-pollutant removal model and the PCA2-cellular constituent model, respectively. Briefly, the study discloses that the cyanobacterium has huge biotechnological and industrial importance as it bioremediates wastewater and simultaneously produces thermostable exopolysaccharide.

**Keywords** Bioremediation · Biosorption kinetics · Cyanobacteria · Pollutants removal model · Polyphasic · Potentially toxic elements

## Introduction

Water contamination is the global problem and its management and treatment have emerged as an escalating challenge globally. Release of untreated industrial and municipal wastes containing toxic pollutants such as dyes, heavy metals, surfactants, herbicides, pesticides, fertilizers and pharmaceuticals into the surface water bodies and their subsequent leaching to the subsoil layers cause pollution and consequently decrease the water and soil quality. Most of the time, industrial and domestic wastewaters are released in the same sewer, making its management more tedious. To overcome the challenges associated with the management of

---

Responsible Editor: Ta Yeong Wu

✉ Satya Shila Singh  
satyashila@rediffmail.com

<sup>1</sup> Laboratory of Cyanobacterial Systematics and Stress Biology, Department of Botany, Banaras Hindu University, Varanasi 221005, India

<sup>2</sup> Laboratory of Microbial Genetics, Department of Botany, Banaras Hindu University, Varanasi, India

mixed type wastewater, various techniques such as chemical (electrochemical oxidation), physical (adsorption and membrane filtration) and biological (using microorganisms) have so far been developed (Crini and Lichtfouse 2019). Although the chemical and physical techniques are rapid and more efficient, they require high energy, maintenance and operational cost. Hence, these techniques are not feasible for small industries. In contrast, the biological techniques are eco-friendly and allow treatment “in situ” which significantly reduces technology cost (Crini and Lichtfouse 2019).

Biological techniques mainly use microorganisms as they provide different mechanisms and pathways of transformation and transfer of hazardous substances from one medium to another. Moreover, their ubiquity, small size, high rate of reproduction and large surface-to-volume cell ratio also make them potential biological agents for wastewater bioremediation. These features are also characteristic for cyanobacteria—one of the oldest groups of photosynthetic prokaryotes on the Earth (Cepoi et al. 2016). Cyanobacteria have big advantages over other life forms, which allowed them to survive in different conditions. Their biochemical processes and specific adaptations under harsh conditions make them very flexible. Moreover, their high availability and autotrophic mode of nutrition are the additional advantages which significantly curtail the cost of industrial cultivation. Besides, cyanobacteria are also well known for their incredible efficiency to adsorb and accumulate potentially toxic elements from the polluted environments (De Philippis et al. 2011). This bioaccumulation of toxic elements by cyanobacteria mainly results from their chelation and incorporation in specific organic structures like amino acids, oligopeptides, proteins and oligo- and polysaccharides (Banerjee et al. 2021). Among these organic compounds, cyanobacterial polysaccharides, especially those which are released outside the cell (exopolysaccharides (EPSs)), have recently gained immense importance as potential biological agents for the treatment of wastewater because they have unique advantages over the EPSs synthesized by plants, animals, and higher algae (Banerjee et al. 2021). The exo or released polysaccharides of cyanobacteria are generally polyanionic heterocyclic compounds rich in uronic acid residues (glucuronic acid and galacturonic acid) and sulfates (De Philippis et al. 2011). In addition to their roles in heavy metal scavenging, EPSs also help cyanobacteria in surface attachment, colonization (Janczarek et al. 2015), and nutrient uptake (Kalpana et al. 2018). However, the production of EPSs is more common in case of those cyanobacterial (López-Ortega et al. 2021) strains which grow under harsh environmental conditions such as high salinity, acidity and temperature. This is so because they use EPS as protective machinery under such tough conditions (López-Ortega et al. 2021). Since EPSs are able to remove both potentially toxic elements and organic pollutants from the environment,

cyanobacterial strains regularly or occasionally exposed to extreme conditions appear to be the most suitable ones for wastewater bioremediation uses. In addition, EPSs produced by these cyanobacterial strains also have biotechnological advantages over traditionally used biopolymers (Arias et al. 2020a). Previously, many studies were performed using cyanobacteria for the wastewater bioremediation (Arias et al. 2020b; Chevalier et al. 2000; Zhu et al. 2021; Samiotis et al. 2022), but most of the studies were conducted in synthetic wastewater using mesophilic cyanobacterial strains. Therefore, studies related to the treatment of natural mixed wastewater using extremophilic EPS-producing cyanobacteria are still vacant despite their remarkable ecological and biotechnological importance.

Among the extreme environments, hot water springs represent a unique habitat where cyanobacteria constitute the major portion of the photosynthetic microbial mats and act as primary producers. In India, about 340 hot springs are known to be present in different ecological regions but only few hot springs especially located in the northern part of India have so far been investigated for their cyanobacterial diversity. Furthermore, whatever cyanobacterial strains have been isolated and characterized from these hot springs have not yet been thoroughly studied for their efficiency to bioremediate wastewater and produce EPSs. Thus, cyanobacterial diversities of majority of the Indian hot springs are still remaining largely unexplored. Tatapani hot spring located in the state Chhattisgarh is one such completely unexplored hot spring which presents high possibility of getting new cyanobacterial species (Jaiswal et al. 2021) with interesting properties including bioremediation of polluted environments and EPS production.

In this context, the current study has been designed to isolate a potent cyanobacterial strain from the Tatapani hot spring and assess its ability to bioremediate mixed-type wastewater. Moreover, the additional aims of the study were to assess the ability of the organism to produce EPSs as bio-products and analyze their basic characteristic features for enumerating their biotechnological or industrial prospects. Therefore, the study would not only explore the applicability of the isolated cyanobacterium in wastewater treatment plants but also reflect its prospects in the EPS producing industries.

## Materials and methods

### Sample collection, isolation and purification

The cyanobacterial samples were collected in pre-sterilized falcon tubes from the outflow of Tatapani Hot Spring, Balrampur, Chhattisgarh, India (23.6986°N and 83.68404°E), in May, 2019. The collected samples were repeatedly washed

in double-distilled water to remove sediments and further, isolation and purification was achieved by spreading serially diluted samples on solid BG-11<sub>0</sub> medium (Rippka et al. 1979) and alternative sub-culturing between liquid and solid BG-11<sub>0</sub> medium, respectively. The purified cyanobacterium strain (labeled as TPJ-3) was maintained in liquid BG-11<sub>0</sub> medium (pH 7.6) under the illumination of cool fluorescent light at 50–55  $\mu\text{E m}^{-2} \text{s}^{-1}$  with a photoperiod of 12/12 h light/dark cycle at  $27 \pm 2$  °C.

### Morphological, molecular and phylogenetic analysis of TPJ-3

The morphological attributes like shape, size and position of vegetative cells and heterocytes, branching pattern, presence/absence and color of sheath of isolated cyanobacterium were studied throughout the experiment and for the primary identification of the strain keys of Desikachary (Desikachary 1959) and Komárek (Komárek et al. 2013) were consulted.

Further, for the molecular characterization of TPJ-3, genomic DNA was extracted by using HiPurA Bacterial Genomic DNA Purification Kit (MB505-250R). The cyanobacterial specific primer pA (5'-AGAGTTTGATCC TGGCTCAG-3') and B23S (5'-CTTCGCCTCTGTGTGCCT AGGT-3') were used for the amplification of the 16S rRNA gene and 16S-23S ITS regions (Edwards et al. 1989; Gkelis et al. 2005). The amplified products were sequenced by Sanger's method on a 3730xl DNA analyzer (Applied Biosystems, Foster City, CA, USA) and the obtained sequence was compared with the NCBI database using BLAST tool (<https://blast.ncbi.nlm.nih.gov/Blast.cgi>).

After that, the phylogenetic analysis of the test cyanobacterium was done by retrieving the reference sequences of 16S rRNA gene representing 274 OTUs from the GenBank and aligning using ClustalW in MEGA5.2. Maximum Likelihood (ML), Neighbor-Joining (NJ) and Maximum Parsimony (MP) algorithms were used for the reconstruction of the phylogeny of the strain TPJ-3 in MEGA 5.2 by selecting the model with the lowest Bayesian Information Criterion score (Tamura et al. 2011). The ML tree was inferred using Kimura 2-parameter model (K2 + G + I) and the reliability of all the trees was tested using the bootstrap method with 1000 replicates. The Mfold web server (Zuker 2003) was used for the analysis of folded secondary structure of 16S-23S ITS regions (D1-D1' and box-B) and compared with phylogenetically related taxa.

### Experimental design for wastewater bioremediation

In order to perform wastewater bioremediation study, the Assi Nala which is situated about 1.5 km away from the Assi bank of river Ganga in Varanasi, India, was selected

as sample collection site because it receives untreated domestic as well as industrial effluents regularly. Earlier studies showed that the wastewater of Assi Nala contains high concentrations of toxic (organic and inorganic) pollutants (Singh 2011) and releases them into the river Ganga. Since the river Ganga has a religious background, people of Varanasi as well as from other parts of India frequently uses its water for bathing and drinking purposes which clearly suggests that the Assi Nala is a serious threat to the well-being of Indians and efforts must be invested for the management of its wastewater to minimize its health risks. Therefore, selecting Assi Nala as the wastewater collection site in our study appears to be quite convincing from the view point of wastewater bioremediation research. Wastewater was initially collected from the Assi Nala, Varanasi, India, and further its physico-chemical analysis was performed as per standard protocols (mentioned below). The collected wastewater sample was left for the sedimentation of suspended particles followed by divided into three parts, i.e., (1) un-autoclaved and un-inoculated wastewater (T1), (2) autoclaved wastewater with 0.5  $\text{g L}^{-1}$  inoculum of TPJ-3 strain (T2) and (3) un-autoclaved wastewater with 0.5  $\text{g L}^{-1}$  inoculum of TPJ-3 (T3). Treatment of the autoclave or unautoclaved wastewater with or without the test cyanobacterium was run in 2 L Erlenmeyer flasks under illumination of cool fluorescent light approximately 50–55  $\mu\text{E m}^{-2} \text{s}^{-1}$  with a photoperiod of 12/12 h light/dark cycle at  $27 \pm 2$  °C. Changes in physicochemical properties (pH, total dissolve solid, conductivity, salinity and total hardness), nutrient contents (phosphate, sulfate, nitrate, nitrite, ammonia and chloride) and metal ion concentration (Zn, Ni, Na, Ca and K) of the wastewater were recorded on the 0th, 10th and 20th day under T1, T2 and T3 conditions. Afterwards, the morphological, physiological and biochemical features of the TPJ-3 strain were studied under wastewater grown conditions (T2 and T3) and compared with that of a control condition, i.e., TPJ-3 grown in BG-11<sub>0</sub> medium.

### Measurement of pH, TDS, conductivity, salinity and total hardness

The changes in pH, total dissolved solids, conductivity and salinity in T1, T2 and T3 conditions on the 0th, 10th and 20th day were determined by using PCSTestr 35, whereas the total hardness of the wastewater was measured by titration against EDTA as per described in APHA (APHA 2005).

### Assessment of nutrients and potentially toxic element removal efficiency

The nutrients and potentially toxic element removal ability of TPJ-3 was determined on the 0th, 10th and 20th day by centrifuging cyanobacterium cultures from T1, T2 and T3

at 6000 rpm for 10 min. The obtained supernatants were subjected for the determination of nutrients like phosphate, sulfate, ammonia and chloride contents (APHA 2005). Phosphate and sulfate contents were measured by using vanadomolybdo-phosphoric acid colorimetric method (using  $K_2HPO_4$  as standard) and  $BaCl_2$  turbidity method, respectively. Ammonia was quantified by using Nessler's reagent, whereas chloride content was measured according to the Mohr's method by titrating against  $AgNO_3$  in the presence of potassium chromate as an indicator. Nitrate content was measured by using nitration of salicylic acid method (Cataldo et al. 1975), whereas nitrite content was determined by formation of a reddish purple azo-dye produced by coupling of diazotized sulfanilamide with N-(1-naphthyl)-ethylenediamine dihydrochloride using  $NaNO_2$  as standard (APHA 2005). The concentrations of metal ions (Zn, Ni, Na, Ca and K) in the obtained supernatants were measured by using atomic absorption spectrometer (AAS).

### Biosorption kinetics and distribution of potentially toxic elements (Zn and Ni)

Biosorption assay and cellular distribution of the Zn and Ni were performed by inoculating  $0.5\text{ gL}^{-1}$  biomass of TPJ-3 to autoclaved wastewater (T2). The content was filtered through Whatmann filter paper ( $0.45\text{ }\mu\text{m}$ ) and the concentrations of the Zn and Ni ions were determined at time intervals of 0, 1, 2, 4, 8, 16, 24, 48 and 72 h by using AAS. In order to measure the surface-bound metal ion concentration, wastewater-treated cyanobacterial cells were suspended and vortexed in  $0.1\text{ M HCl}$  for 15 min and then centrifuged at 5000 rpm for 10 min. The obtained supernatant was further analyzed through AAS to measure the concentration of Zn and Ni and the remaining cyanobacterial pellet was used for measuring the intracellular concentrations of the same metals. For this, the cyanobacterial pellet was acid digested ( $HNO_3$ :  $HCl$ , 1:3 v/v) and the obtained solution was diluted using metal-free double-distilled water and then analyzed to estimate the intracellular concentrations of Zn and Ni.

The metal biosorption efficiency and maximum biosorption capacity at equilibrium was calculated according to the following equations:

$$\text{Biosorption efficiency (\%)} = \frac{(C_0 - C_e)}{C_0} \times 100$$

$$\text{Biosorption capacity (qt)} = \frac{(C_0 - Ct)V}{M}$$

$$\text{Biosorption capacity (qe)} = \frac{(C_0 - C_e)V}{M}$$

where  $q_t$  is the biosorption capacity at time  $t$  ( $\text{mg g}^{-1}$ ),  $q_e$  is the biosorption capacity ( $\text{mg L}^{-1}$ ) at equilibrium,  $C_0$  is the initial metal ion concentration ( $\text{mg L}^{-1}$ ),  $C_t$  is the metal ion concentration ( $\text{mg L}^{-1}$ ) at time  $t$ ,  $C_e$  is the metal ion concentration ( $\text{mg L}^{-1}$ ) at equilibrium,  $V$  is the volume of the medium (L) and  $M$  is the amount of the bio-sorbent (g). The Langergren linearized form of the pseudo-first-order and pseudo-second-order adsorption kinetic equation (Ramesh et al. 2012) used was described below:

$$\log(q_e - q_t) = \log q_e - \frac{k_1 t}{2.303}$$

$$\frac{t}{q_t} = \frac{1}{k_2 q_e^2} + \frac{t}{q_e}$$

where  $k_1$  is the rate constant of pseudo-first-order adsorption and  $k_2$  is the rate constant of pseudo-second-order adsorption.

### Determination of changes in morphological, physiological and biochemical attributes of TPJ-3

#### Characterization of morphological changes

The changes in size and shape of vegetative cells and heterocytes as well as frequency of heterocytes were observed using the microscope (Olympus CX43 fitted with Magnus magCam DC-5 camera) under wastewater (T2 and T3) and control condition (BG-11<sub>0</sub>). The permeabilized cells were stained with DAPI (4',6-diamidino-2-phenylindole) and further visualized under the confocal microscopy (Zeiss LSM-780) to detect intracellular changes using the excitation filter at 370 nm and emission filter at 526 nm (Mukherjee et al. 2015).

#### Estimation of chlorophyll *a* (chl *a*) and biomass

The growth of the strain TPJ-3 in terms of the chl *a* was estimated on the 0th, 5th, 10th, 15th and 20th day. 5 mL of cyanobacterial culture was harvested from BG-11<sub>0</sub>, T2 and T3 by centrifugation at 6000 rpm for 10 min and washed twice with double-distilled water. The pellets were resuspended in 5 mL of 95% methanol and kept overnight at  $4\text{ }^\circ\text{C}$  in dark. The  $A_{665}$  and  $A_{720}$  of the supernatants were recorded using spectrophotometer (Hitachi U-2900) and the chl *a* was calculated according to the Ritchie (Ritchie 2006) and expressed in terms of  $\mu\text{g mL}^{-1}$ .

The changes in biomass production of TPJ-3 in terms of fresh weight was obtained on the 0th, 10th and 20th day by weighing the blot dried cyanobacterial culture from BG-11<sub>0</sub>, T2 and T3 using microbalance (Shimadzu AUX 220) and represented as  $\text{gm L}^{-1}$ .

## Estimation of protein, lipids and carbohydrate

The protein content was measured by centrifuging the cyanobacterial cultures from BG-11<sub>0</sub>, T2 and T3 on the 0th, 10th and 20th day at 6000 rpm for 10 min. The obtained pellets were washed and resuspended in potassium phosphate buffer (pH 6.8, 50 mM) and then crushed in liquid nitrogen with the help of mortar and pestle. After centrifugation at 12,000 rpm for 15 min at 4 °C, the protein content was measured according to the protocol of Bradford (Bradford 1976) by taking absorbance at 595 nm and using BSA standard.

For the extraction of total lipids from TPJ-3 on the 0th, 10th and 20th day from BG-11<sub>0</sub>, T2 and T3 the cyanobacterial cells were crushed in chloroform:methanol (2:1 v/v) using mortar and pestle. Then, equal volume of distilled water was added and after 10 min of incubation at room temperature centrifuged at 6000 rpm for 10 min. After achieving phase separation, the upper phase, i.e., aqueous, was discarded whereas the lower phase chloroform was used for total lipid. The dissolved lipids in chloroform were determined by the method described by Yi and Jean (2011) using canola oil as standard. The estimation of carbohydrate content of TPJ-3 in BG-11<sub>0</sub>, T2 and T3 was done by the phenol–sulfuric acid method using glucose as standard as per the protocol given by Dubois (Dubois et al. 1951).

## Extraction and quantification of capsular and released exopolysaccharides

The extraction of EPS was performed as per the protocol described by Khattar (Khattar et al. 2010) with some modification. For the capsular EPS, cyanobacterial cultures were harvested from BG-11<sub>0</sub>, T2 and T3 on the 0th, 10th and 20th day by centrifugation at 6000 rpm for 10 min and the obtained pellets were treated with a mixture of 0.6 M NaCl and 0.06 M EDTA at 65 °C for 3 h followed by cooling at RT. Further, centrifugation was performed at 10,000 rpm for 20 min and the obtained supernatants and cell free medium (for released EPS) were treated with equal volume of chilled ethanol and kept at 4 °C overnight. The precipitated EPS was centrifuged at 10,000 rpm for 20 min and washed twice with chilled 96% ethanol. Thereafter, the pellet was air-dried for removal of any residual ethanol and sample was stored at –20 °C for further analysis. The carbohydrate content in the EPS was quantified by the phenol–sulfuric acid method using the protocol given by Dubois (Dubois et al. 1951). After that, the protein content in EPS was also measured by Bradford protein assay (Bradford 1976). In our study, the released EPS content was found to be extremely low ( $0.099 \pm 0.002$ ,  $0.103 \pm 0.002$  and  $0.150 \pm 0.015$  mg g<sup>-1</sup> FW in BG-11<sub>0</sub>, T2 and T3 conditions respectively); henceforth, the capsular EPS was further characterized and designated as EPS.

## Fourier transform infrared spectroscopy and thermogravimetric analysis of EPS

The chemical compositions of EPS were determined via Fourier transform infrared spectroscopy (FTIR) spectrophotometer (PerkinElmer Spectrum Version 10.03.05) where 1 mg of EPS was grounded with 100 mg of potassium bromide (KBr) powder and then compressed into pellets of 3-mm diameter. Fourier transform infrared spectrum was then acquired in transmittance mode to analyze different functional groups in the frequency range of 4000–400 cm<sup>-1</sup>.

Thermogravimetric analysis (TGA) of EPS was carried out on PerkinElmer STA 6000 where TGA curve plots the reference material temperature on the *x*-axis against the TGA signal, converted to percentage weight change on the *y*-axis. For the analysis, EPS was placed in a platinum crucible and heated at a linear rate of 10 °C min<sup>-1</sup> over a temperature range of 30 to 700 °C under nitrogen environment and the corresponding weight loss was determined.

## Metal-binding analysis of the EPS

The metal-binding capacity of the EPS was analyzed by equilibrium dialysis experiment as described previously (Geddie and Sutherland 1993; Morillo et al. 2006). The experiment was performed in 200 ml of 0.1 mM solution of the metal ion (Ni, Zn, Co, Cd and Cu) separately as well as in mixed condition. Five milliliters of EPS solution in milli Q water (0.5% w/v) was placed into the pre-treated dialysis tube (Himedia-LA395, 12,000 Da) and was released into the flask containing 200 mL of the respective metal ion solution under shaking condition (100 rpm) at room temperature. The concentration of the metal ions was measured at 0 and 24 h by using AAS.

## GC–MS analysis of fatty acid methyl esters

The cyanobacterial cells from BG-11<sub>0</sub> and T2 were harvested on the 20th day and 1 g dried cells was crushed in appropriate amount of chloroform:methanol (2:1 v/v) followed by saponification and methylation by sodium methoxide and boron trifluoride-methanol, respectively, and boiled for 12 min. The sample was immediately cooled on ice bath followed by addition of 5 mL of HPLC grade *n*-hexane (Kang and Wang 2005). After layer separation, 2/3<sup>rd</sup> of upper hexane layer was transferred to GC vials and concentrated until 100 µL samples were remained. Finally, 3 µL of sample was injected to GC–MS for the analysis of fatty acids.



## Statistical analysis

All the experimental results were represented as the means of three replicates and were statistically analyzed at 95% significance level by two-way ANOVA (Tukey test) using IBM SPSS statistics 26. To determine the effect of cultivation time, various conditions, and their correlation with the cellular constituents as well as the nutrient and metal ion contents in wastewater, the principal component analysis (PCA) was performed using XL STAT software.

## Results and discussion

### Morphological, molecular and phylogenetic analysis

Strain TPJ-3 formed conspicuous soft spongy, bluish green to brownish green mat attached to the substratum on running shallow water at the time of sampling. In-depth microscopic observation the strain showed typical characteristics of the family Scytonemataceae. The filaments were densely entangled, uniseriate, isopolar and depicted single and geminate type of false branching. Filaments were enclosed in firm, distinct and colorless sheath. The barrel-shaped vegetative cells of filament were usually wider than length where length and width were found to be ranged from 6.00 to 10.00  $\mu\text{m}$  and 8.50 to 12.00  $\mu\text{m}$  respectively (Fig. 1). The terminal cell of the filaments was interestingly always yellowish in color with rounded end. The intercalary positioned heterocytes were solitary as well as paired with concave and convex type of ends whereas length and width ranged from 10.50 to 30.00  $\mu\text{m}$  and 10.00 to 13.00  $\mu\text{m}$  respectively. Akinetes were not observed throughout the study. The morphological characters of the strain TPJ-3 were compared with the other *Scytonema* species (Table S1). The presence of terminal yellowish cell with rounded end and comparatively larger, solitary and paired heterocytes with concave and convex ends seems interesting.

Further, the identity of TPJ-3 was resolved by molecular characterization for which the partial sequence (1494 bp) of 16S rRNA gene was obtained and its comparative BLAST analysis amongst 16S rRNA gene sequences in GenBank showed 96.68% similarity with the strain *Scytonema* cf. *mirabile* ER0515.01 (MG970546). The pairwise comparison of the strain TPJ-3 with putatively related taxa showed that they shared less than 96.60% similarity (Table S2). Thus, the identity of TPJ-3 as *Scytonema* was established and also, the possibility of TPJ-3 as new member of genus *Scytonema* was suggested.

Additionally, the phylogenetic tree reconstructed from 274 nucleotide sequences of the 16S rRNA gene depicted the stable clustering of TPJ-3 within the *Scytonema* clade on separate node with strong bootstrap support

(99/100/99), and consistent tree topology (Fig. 2) provided strength to the proposition of TPJ-3 as new species of genus *Scytonema*. The sequences of *Scytonema* were clustered into multiple groups which represented the polyphyly of the genus *Scytonema* as shown in previous studies (Komárek 2013; Mishra et al. 2021; Saraf et al. 2018). Members of these clusters may represent new generic identities; hence, their further study using polyphasic approach is essential before creating new generic identities. The families Tolypothrichaceae and Godleyaceae form monophyletic clades unlike the highly polyphyletic family Scytonemataceae which suggested that the intense revision at family level is indispensable.

Further, the taxonomic validation of TPJ-3 was achieved by secondary structure analysis of 16S-23S ITS region. The folded structure of D1-D1' helix was compared with closely related taxa *S. panchmarhiense* and *S. javanicum* (Fig. S1) and showed a deferent folding pattern. The D1-D1' helix of TPJ-3 comprised 97 nucleotides and showed continuous formation of two topmost loops whereas in *S. panchmarhiense* and *S. javanicum*, D1-D1' helix consisted of 102 and 82 nucleotides with no single topmost loops. Further, the folded structure of box-B region of strain TPJ-3 also differed from *S. panchmarhiense* and *S. javanicum* by having only 29 nucleotides instead of 31 and contained a small loop of 6 nucleotides at the top instead of 12 and 8 nucleotides as in *S. panchmarhiense* and *S. javanicum*, respectively (Fig. S2).

The polyphasic evaluation and comparative analysis of strain TPJ-3 using morphological, molecular phylogenetic (16S rRNA based) and folded secondary structures of ITS regions indicated that the strain is indeed a new member of the genus *Scytonema*.

### Bioremediation of wastewater by TPJ-3

#### Physicochemical characteristics of wastewater collected from Assi Nala, Varanasi, India

The results obtained from the physicochemical analyses of wastewater revealed that the water was highly contaminated with phosphate, sulfate, nitrogen (nitrate, nitrite, and ammonium), Cl, Na, Ca, K, Zn, Ni, Cu, Cr and Cd (according to the permissible limit, WHO). The presence of these pollutants collectively indicated the toxicity and mixed nature of the wastewater (Table 1). Although it is well known that the abundance of phosphate and nitrogen in water causes eutrophication, no micro-algal growth was observed both at the sampling site and in laboratory (T1). Along with excessive nutrients, the presence of potentially toxic elements was supposed to be the reason of such observation.

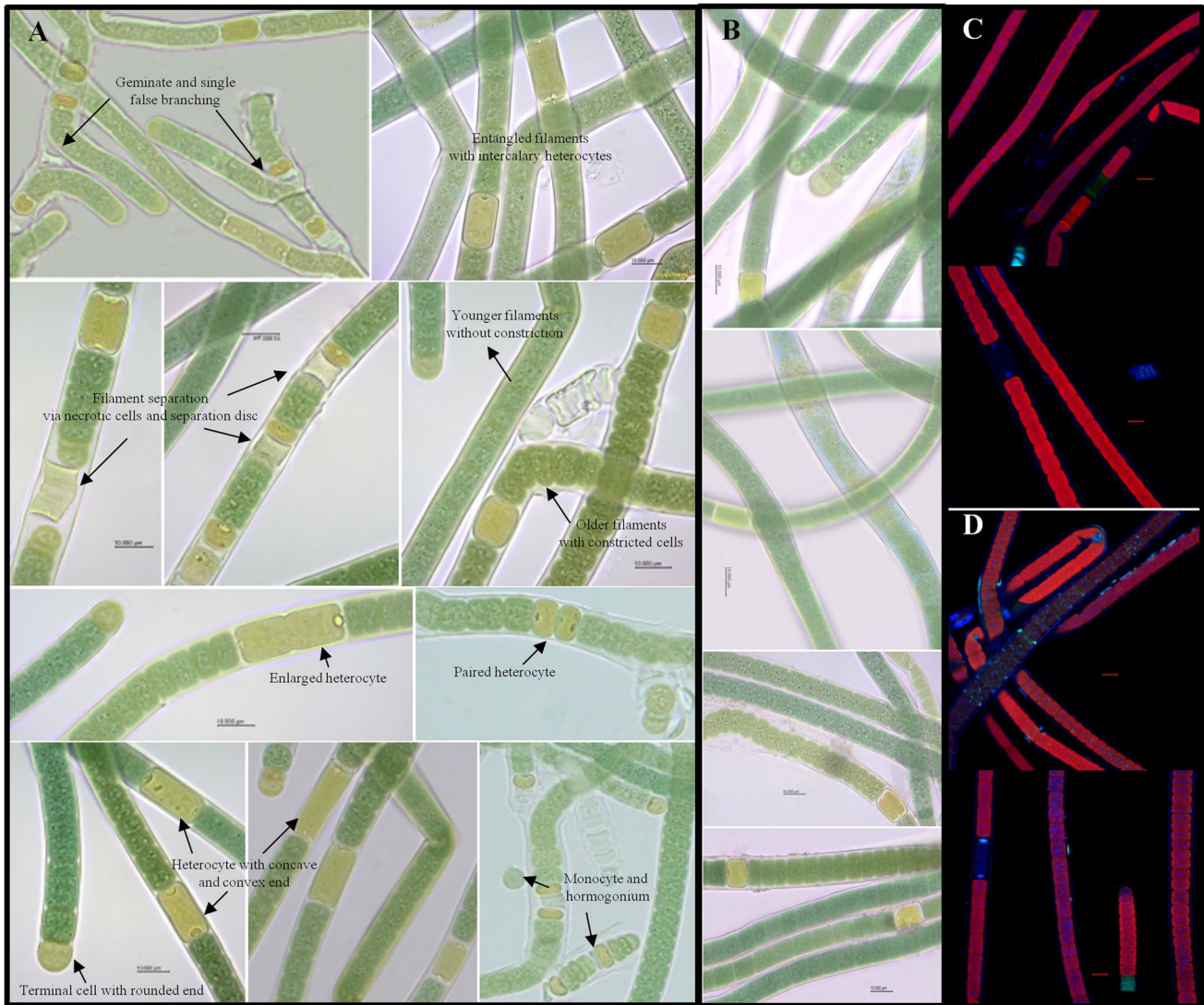


**Fig. 1** Morphological attributes of *Scytonema* sp. TPJ-3 and comparison between standard media (BG-11<sub>0</sub>)-grown and wastewater-grown culture. Scale bar 10 µm. (A) *Scytonema* sp. TPJ-3 grown in BG-11<sub>0</sub>,

(B) *Scytonema* sp. TPJ-3 grown in wastewater, (C) DAPI-stained strain *Scytonema* sp. TPJ-3 grown in BG-11<sub>0</sub>, and (D) DAPI-stained strain *Scytonema* sp. TPJ-3 grown in wastewater

### Removal of pollutants by TPJ-3 and changes in physicochemical properties of the wastewater

After the growth of strain TPJ-3 in wastewater conditions, the conductivity, TDS, salinity, and hardness of the wastewater were found to be decreased whereas the pH was recorded to be increased significantly ( $p$  value > 0.001) (Table 2). Conductivity was decreased from 395.00 to 248.50 µS in T3 condition and from 391.00 to 269.50 µS in T2 conditions on the 20th day while TDS was dropped from 282.00 to 178.50 mg L<sup>-1</sup> in T3 condition and from 278.00 to 191.00 mg L<sup>-1</sup> in T2 condition. Salinity was curtailed by 37% in T3 condition, 32% in T2 condition, and 25% in BG-11<sub>0</sub> condition on the 20th day. Reduced salinity and conductivity of the wastewater may be corroborated

with the removal of mainly Na, K and Ca ions by 20% and 28%, 81% and 90%, and 80% and 90% respectively in T2 and T3 conditions on the 20th day by TPJ-3. Moreover, the declined level of TDS may be attributed to the degradation of dissolved solids by TPJ-3 into simpler forms followed by their possible utilization as nutrients. The total hardness, which was observed to be minimized significantly, i.e., from 211.33 to 67.33 mg L<sup>-1</sup> and 53.33 mg L<sup>-1</sup> in T2 and T3 conditions respectively (Table 2,  $p$  value > 0.001), may also be connected with efficient removal of nutrients and metal ions from the wastewater by the TPJ-3 strain. However, the increase in pH of the wastewater from 8.50 to 10.07 and 9.89 in T2 and T3 conditions was recorded respectively. The increased pH may be ascribed to the cyanobacterial carbon concentration mechanism because

**Fig. 2** Phylogenetic position of strain TPJ-3 based on 16S rRNA gene along with 274 OTUs of heterocytous genera inferred by Maximum Likelihood tree with the bootstrap values representing ML/NJ and MP, respectively. Bar 0.05 changes per nucleotide position

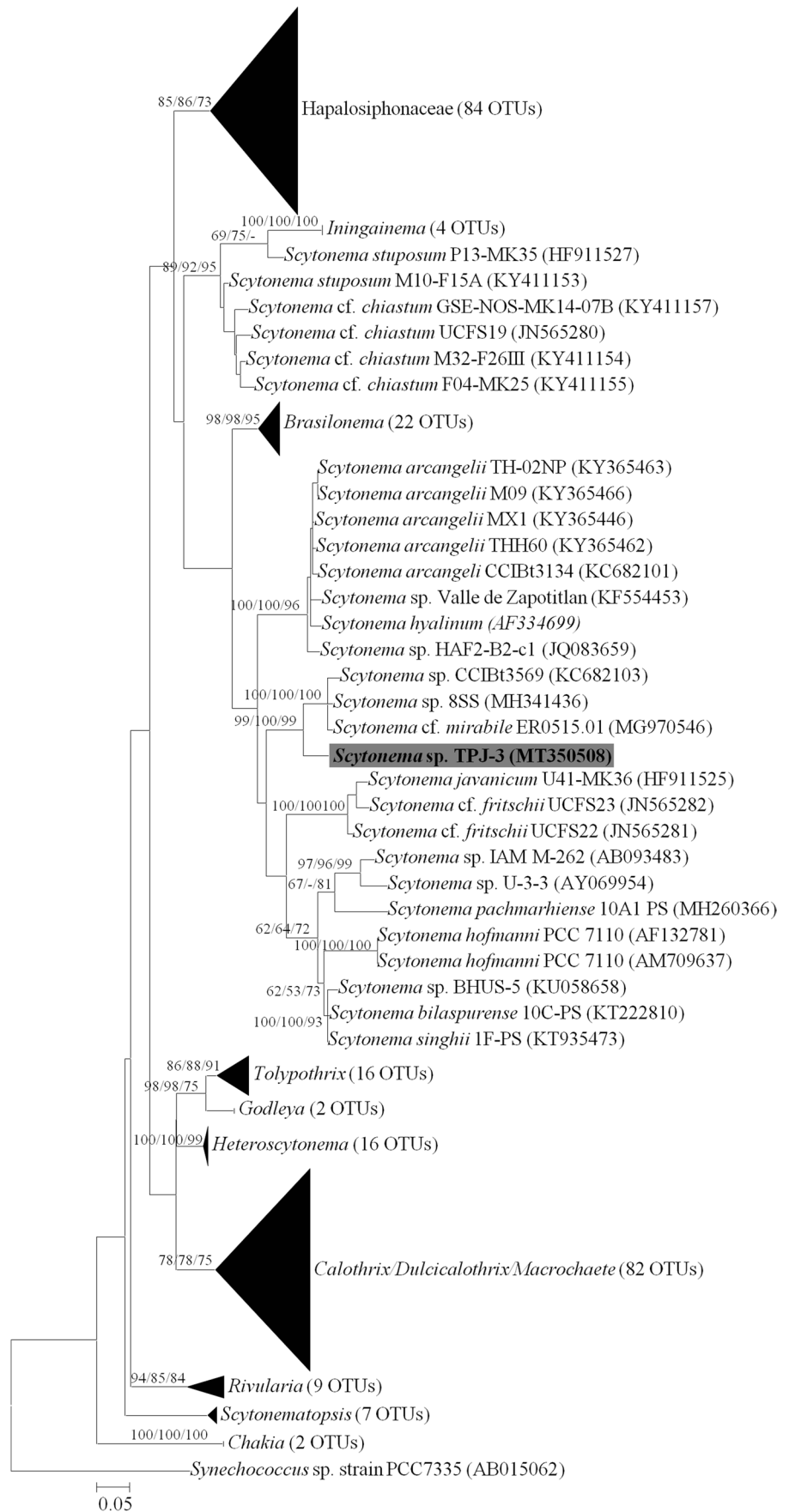




**Table 1** Physicochemical analysis of the wastewater

Parameters		Permissible limits (WHO)
pH	8.57 ± 0.03	6.5–8.5
Conductivity (µS)	396 ± 1.41	–
Salinity (mg L <sup>-1</sup> )	195.50 ± 1.06*	60
Total dissolved solids (mg L <sup>-1</sup> )	284 ± 0.70	500
Hardness (mg L <sup>-1</sup> )	211.33 ± 2.30*	200
Phosphate (mg L <sup>-1</sup> )	245.79 ± 20.07*	0.1
Sulfate (mg L <sup>-1</sup> )	37.58 ± 1.75	200
Nitrate (mg L <sup>-1</sup> )	218.67 ± 7.02*	45
Nitrite (mg L <sup>-1</sup> )	127.87 ± 4.35*	–
Ammonia (mg L <sup>-1</sup> )	14.45 ± 1.25*	0.5
Chloride (mg L <sup>-1</sup> )	234.30 ± 3.55	250
Zinc (mg L <sup>-1</sup> )	18.52 ± 0.17*	5
Nickel (mg L <sup>-1</sup> )	0.94 ± 0.15*	0.02
Sodium (mg L <sup>-1</sup> )	112.15 ± 3.78*	50
Potassium (mg L <sup>-1</sup> )	31.30 ± 0.26*	10
Calcium (mg L <sup>-1</sup> )	29.22 ± 2.77	75
Copper (mg L <sup>-1</sup> )	0.02 ± 0.003	0.05
Iron (mg L <sup>-1</sup> )	0.30 ± 0.09	0.3
Cadmium (mg L <sup>-1</sup> )	0.08 ± 0.003*	0.003
Chromium (mg L <sup>-1</sup> )	0.04 ± .008	0.05
Bacterial count (CFU mL <sup>-1</sup> )	27 × 10 <sup>4</sup>	–

\*Concentration is above the permissible limit

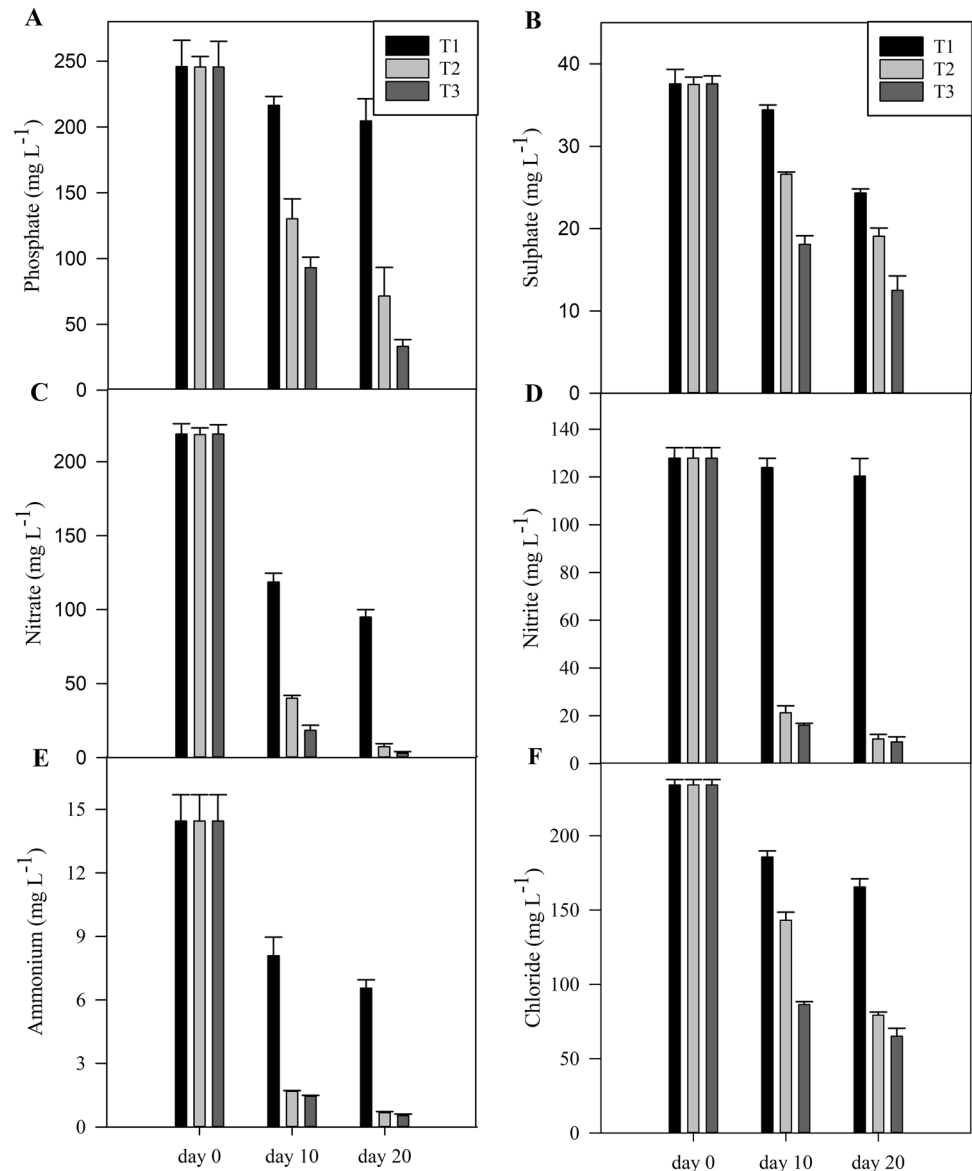
during this process, the photosynthetic dissociation of hydrogen carbonate into CO<sub>2</sub> and OH<sup>-</sup> takes place in carboxysome and the produced OH<sup>-</sup> further gets released outside the cells and increases the pH of the surrounding environment (Kishi et al. 2020). Furthermore, the elevation in pH by the cyanobacterium caused reduction in TDS by precipitating hydroxide ions; this hydroxide ion precipitation was supposed to be the reason why no growth of other invasive microorganisms (bacteria and fungi) was found during this study (Shahid et al. 2020). Since the high concentrations of inorganic phosphorous and nitrogen in wastewater lead to eutrophication, the removal of these two nutrients is an important aspect to mitigate

water eutrophication (Whitton et al. 2016). The nutrient removal ability of the strain TPJ-3 in terms of phosphate, sulfate, nitrate, nitrite, ammonium and chloride is depicted in Fig. 3. The removal of the phosphate content on the 20th day in T2 and T3 conditions was 70% and 86% whereas the sulfate content was decreased by 49% and 66% respectively (Fig. 3A, B). Nearly complete removal of nitrate, nitrite and ammonium, i.e., 96%, 91%, and 95%, in T2 and 98%, 92%, and 96% respectively, by TPJ-3 from the wastewater was recorded on the 20th day (Fig. 3C, D, E). Interestingly, the results of our study reflected that the initial concentrations as well as removal of phosphate, sulfate and nitrogen (nitrate, nitrite and ammonium) was comparatively higher than that observed in the earlier wastewater bioremediation studies performed using cyanobacteria (Bohutskyi et al. 2016; Wu et al. 2018) (Table S4). Additionally, the surplus phosphate in the wastewater induced the intracellular accumulation of poly-phosphate bodies (Sanz-Luque et al. 2020), which was examined in the TPJ-3 cells through confocal microscopy (Fig. 1C, D). The higher concentration of nitrogen and phosphorous sources increases the assimilation of nitrate and phosphate in the biomass (Samiotis et al. 2022) as shown in Fig. 1D and 6B. Further, the elevated removal of zinc and nickel from the wastewater by TPJ-3 strain was also a unique observation of the present study (Fig. 4A, B). While the Zn and Ni concentrations were decreased by 81% and 80% respectively, in T3, 79% and 68% drop respectively in Zn and Ni concentrations was identified in T2. An elevated removal of Zn and Ni from the wastewater by cyanobacteria may be linked to the cyanobacterial ability to adsorb them on the surface by synthesizing EPSs and/or accumulate them inside cells (Chakraborty and Mishra 2020). In order to validate this prediction, we analyzed the Zn and Ni biosorption kinetics in TPJ-3 strain in T2 condition and this study revealed that the cyanobacterium followed pseudo-second-order reaction model of biosorption kinetics for both Zn and Ni as the experimental  $q_e$  ( $q_{e(\text{exp})}$ ) was closer to theoretical  $q_e$  of the pseudo-second-order biosorption kinetics with high correlation coefficient ( $R^2$ ) (Fig. 5). Moreover, the study also unveiled that the rate limiting step was chemisorptions and the rate of the adsorption was dependent on the biomass of

**Table 2** Change in physicochemical properties of wastewater after the inoculation of strain *Scytonema* sp. TPJ-3

Parameter	T1		T2		T3	
	Day 10	Day 20	Day 10	Day 20	Day 10	Day 20
pH	8.75 ± 0.03	8.90 ± 0.04	9.99 ± 0.03	10.07 ± 0.07	9.56 ± 0.05	9.89 ± 0.03
Conductivity (µS)	389 ± 1.41	384 ± 2.83	290 ± 2.83	269.50 ± 2.12	288 ± 2.82	248.5 ± 3.53
Salinity (mg L <sup>-1</sup> )	187 ± 1.41	185 ± 2.12	145.50 ± 2.47	130.50 ± 1.06	140.50 ± 0.35	122 ± 2.12
TDS (mg L <sup>-1</sup> )	277.50 ± 0.35	277 ± 1.41	210.50 ± 1.76	191.50 ± 1.06	205.50 ± 0.35	178.50 ± 1.06
Hardness (mg L <sup>-1</sup> )	160.66 ± 3.05	142.66 ± 2.30	67.33 ± 3.05	53.33 ± 3.05	60 ± 2	40 ± 2

**Fig. 3** Changes in nutrient contents of wastewater under different conditions. (A) Phosphate, (B) Sulfate, (C) Nitrate, (D) Nitrite, (E) Ammonium and (F) Chloride

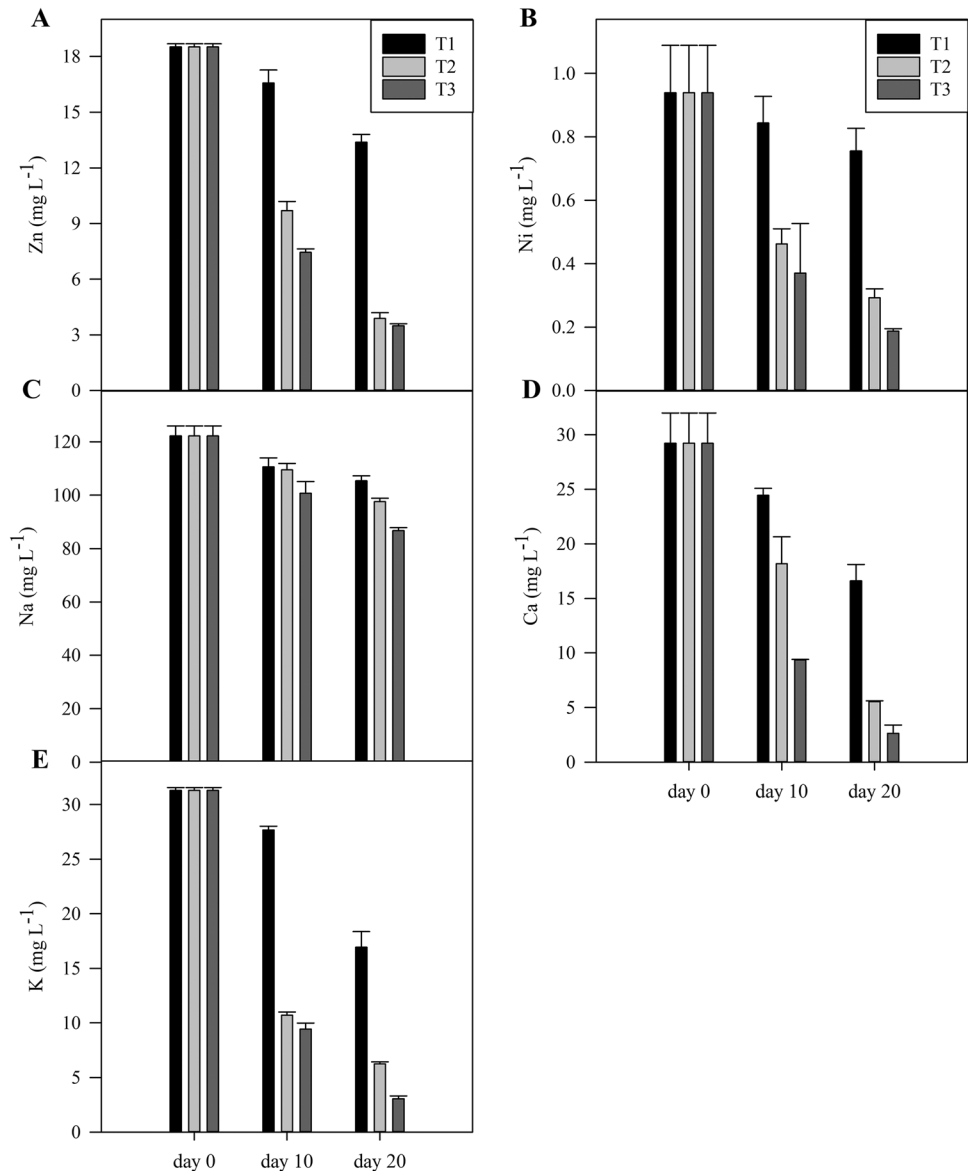


the cyanobacterium TPJ-3. Moreover, the results obtained from the analyses of cellular distribution of Zn and Ni reflected that the cyanobacterium contained  $3.54 \pm 0.08$  and  $0.59 \pm 0.01$  mg L<sup>-1</sup> Zn and Ni, respectively, on its surface and accumulated  $11.05 \pm 0.21$  and  $1.37 \pm 0.10$  mg L<sup>-1</sup> Zn and Ni, respectively, inside the cells (Fig. S3). This indicated that the metal ions were removed by the cyanobacterium from the wastewater through sequential process of adsorption and absorption (Sutherland and Ralph 2019). Although the trace levels of Zn and Ni play an important role in the cyanobacterial physiology by acting as the cofactors of hydrolase and urease enzymes, respectively, the higher concentrations of these trace metals exert deleterious effects on the growth of cyanobacteria (Huertas et al. 2014). In our study, however, the strain TPJ-3 was

found to grow efficiently in presence of high concentrations of Zn and Ni which revealed the highly adaptability of the cyanobacterium.

As compared to T2 (autoclaved TPJ-3 inoculated wastewater), the removal of majority of the pollutants was slightly higher in T3 (unautoclaved TPJ-3 inoculated wastewater). This may be described by the fact that the unautoclaved wastewater sample, i.e., T3, possibly contained other microorganisms along with the test cyanobacterium which ultimately caused enhanced removal of pollutants; however, autoclaving the wastewater might have killed those organisms in T2 and only the cyanobacterium was there which removed slightly lesser amounts of pollutants. Despite these clearly observable differences between T2 and T3 in removing pollutants, it can be firmly said

**Fig. 4** Changes in metal ions concentration from wastewater under different conditions. (A) Zn, (B) Ni, (C) Na, (D) Ca and (E) K



that the test cyanobacterium alone was highly efficient in removing pollutants from wastewater.

### Modulations in morphological and physiological characteristics of TPJ-3

#### Changes in morphological characteristics

Microscopy revealed no changes in size and shape of vegetative cells of TPJ-3 in wastewater (T2 and T3) when compared with that of the BG-11<sub>0</sub> medium. While the filaments remained intact and dark bluish green even after the 15th day of inoculation in wastewater conditions, BG-11<sub>0</sub>-grown cyanobacterial filaments started fragmenting and became slightly yellowish in color (Fig. 1A, B). The sheath became slimy in wastewater condition which was

a result of increased production of EPSs. Moreover, the heterocyte frequency in TPJ-3 was decreased in wastewater conditions from 7.21 to 4.33% in respect to the control as the nitrogen sources were available in surplus amount. Confocal microscopy of cyanobacterial filaments reflected the enhanced accumulation of polyphosphate bodies (PPBs) inside the cells of wastewater grown TPJ-3 as compared to that of the control (BG-11<sub>0</sub> medium) (Fig. 1C, D). The intracellular accumulation of PPBs suggested the excellent uptake of the phosphate by TPJ-3.

#### Changes in cellular constituents

The chl *a* content of the cyanobacterium TPJ-3 was recorded to be increased by 3.86, 4.51 and 4.82 times respectively in BG-11<sub>0</sub>, T2 and T3 on the 20th day.

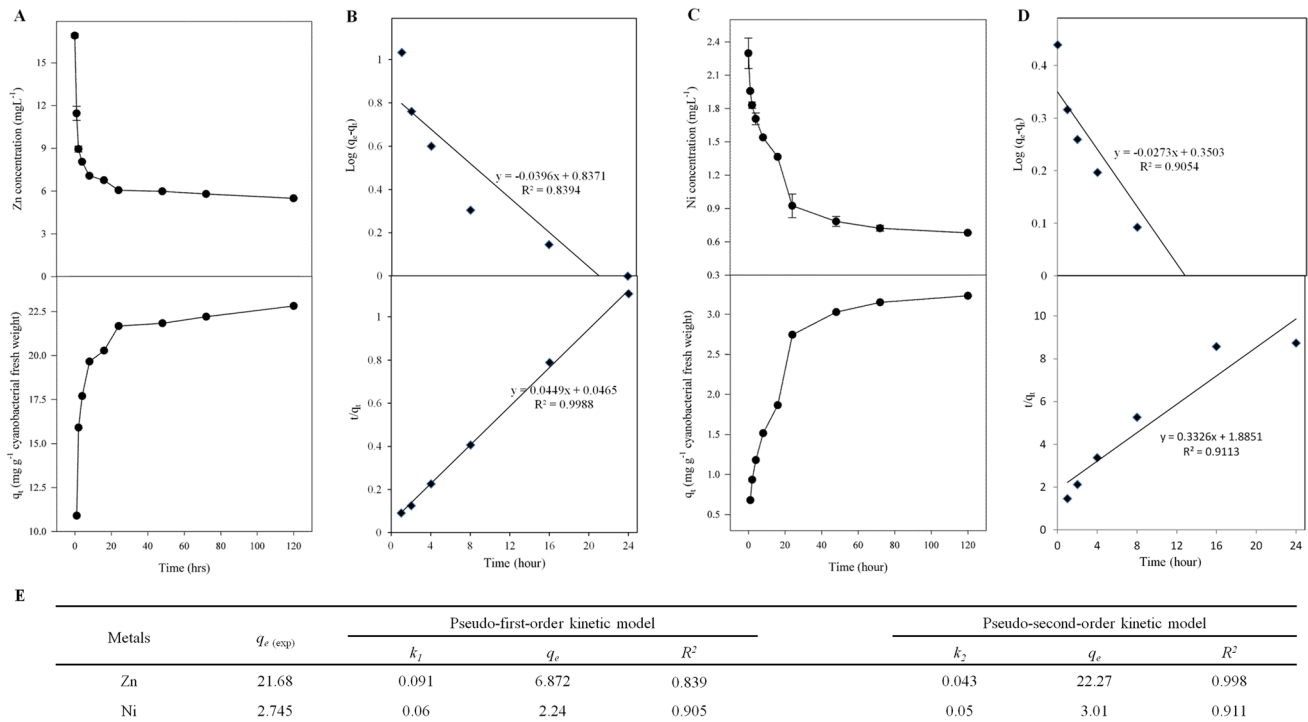


**Fig. 5** Bioabsorption kinetics of heavy metals (A) Zn biosorption, (B) linearized plot the pseudo-first-order and pseudo-second-order adsorption kinetic of Zn, (C) Ni biosorption, (D) linearized plot the pseudo-

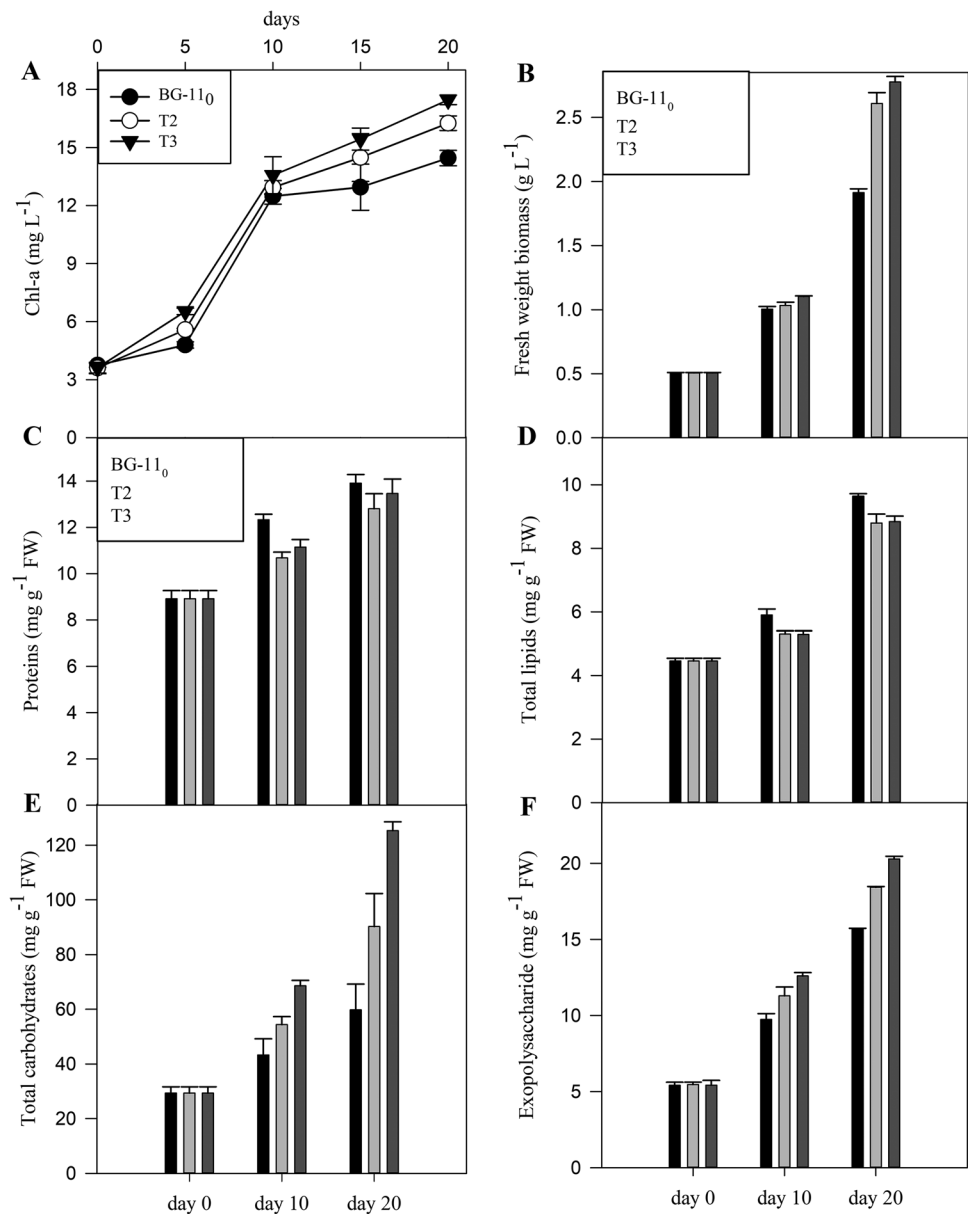
first-order and pseudo-second-order adsorption kinetic of Ni, and (E) comparison of the pseudo-first and pseudo-second-order biosorption rate constants and experimental  $q_e$  ( $q_e$ (exp)) and theoretical  $q_e$  values

Biomass was also increased by 3.78, 5.15 and 5.48 times in BG-11<sub>0</sub>, T2 and T3 respectively. The increment in chl *a* and biomass was found to be up to 1.12 and 1.38 times higher in T2 and 1.21 and 1.71 times higher in T3 when compared with BG-11<sub>0</sub>. This indicated that the highest growth was in T3 and least in BG-11<sub>0</sub> (Fig. 6A, B). The final biomass production of the TPJ-3 under wastewater condition was recorded 2.60 gL<sup>-1</sup> in T2 and 2.77 in T3 which was comparable to the previous reports (Table S4), where biomass production up to 2.00 gL<sup>-1</sup> by *Synechococcus*; 1.50 gL<sup>-1</sup> by *Anabaena*, *Nostoc* and *Calothrix*, (Aketo et al. 2020); 1.88 gL<sup>-1</sup> by *Acaryochloris marina*; and 2.23 gL<sup>-1</sup> by *Oscillatoria* and *Pleurocapsa* has been reported under wastewater condition (Shahid et al. 2020). Thus, it can be speculated that the abundance of nutrients in wastewater supported the growth of the strain or the excellent nutrient uptake capability of the strain TPJ-3 due to its extreme habitat origin could be the reasons of its luxurious growth and higher biomass production in wastewater. The production of such a high amount of biomass in wastewater creates interest to subject the cyanobacterium for further extraction of economically important substances such as biodiesel, biopolymer, exopolysaccharides, pigments and secondary

metabolite production (Arias et al. 2020a; Singh et al. 2019). The result obtained after estimating the protein, carbohydrate and lipid contents indicated drastic change in carbohydrate content of TPJ-3 when grown in wastewater (Fig. 6E). However, no significant alteration was observed in case of protein and lipid contents (Fig. 6C, D). In contrast, the protein and lipid contents were found to be slightly higher in BG-11<sub>0</sub>-grown TPJ-3 with respect to T2 and T3 (Fig. 6C, D). In addition, from the initial day, there were 2.03, 3.07, and 4.27 times increments in total carbohydrate content observed in BG-11<sub>0</sub>, T2 and T3 respectively (Fig. 6E). This suggested that the pollutants present in wastewater acted as stressors and also triggered the osmotic changes due to high salinity of wastewater (about 81% higher than BG-11<sub>0</sub>) which in turn resulted in the increased biomass production with increased carbohydrates level to regulate the inner-cell turgor pressure (Samiotis et al. 2021). This further indicated the allocation of photosynthates toward carbohydrate synthesis and mainly EPSs as the carbohydrates also comprise the EPS that stabilize membrane structure and provide cellular stability; furthermore, the negatively charged EPS reduced the toxicity level by the biosorption of heavy metals (De Philippis et al. 2011).



**Fig. 6** Changes in biomass, cellular constituents and extracellular content of the *Scytonema* TPJ-3 under different conditions. (A) Chlorophyll *a*, (B) Fresh weight biomass, (C) Proteins, (D) Total lipids, (E) Total carbohydrates and (F) Exopolysaccharide



### Production of exopolysaccharides by wastewater grown TPJ-3

Results of EPS content analysis disclosed that there were 2.89, 3.37 and 3.74 times enhancement in EPS content of TPJ-3 on the 20th day under BG-11<sub>0</sub>, T2 and T3 condition respectively (Fig. 6F). This increased production of EPS was supposed to be a mechanism of the cyanobacterium to compensate osmotic changes, survive and grow in the wastewater which was contaminated with the high concentrations of several nutrients and metal ions (Table 1). The inductive effects of combined nitrogen, heavy metals, calcium, pH and salinity on the production of EPS by cyanobacteria have previously been reported by Pereira (Pereira et al. 2011). Since EPS has multifaceted use in food and pharmaceutical industries, this high EPS-producing

ability makes the strain TPJ-3 a perfect platform for the production of EPS at the industry scale (Li et al. 2001).

### Fourier transform infrared spectroscopy analysis of EPS produced by TPJ-3

The outcomes of FT-IR analysis elucidated the biochemical characteristics of the EPS by determining its functional groups (Fig. 7A). The broad spectrum around 3410 cm<sup>-1</sup> (3401 cm<sup>-1</sup> in T2) and sharp ones at 2929 cm<sup>-1</sup> is common to all polysaccharides and corresponds to the stretching vibration of hydroxyl group and C–H, respectively (Kavita et al. 2014). A small band at 2345.27 cm<sup>-1</sup> was found in BG-11<sub>0</sub>, but not in T2, which corresponded to the amine group (Ahluwalia and

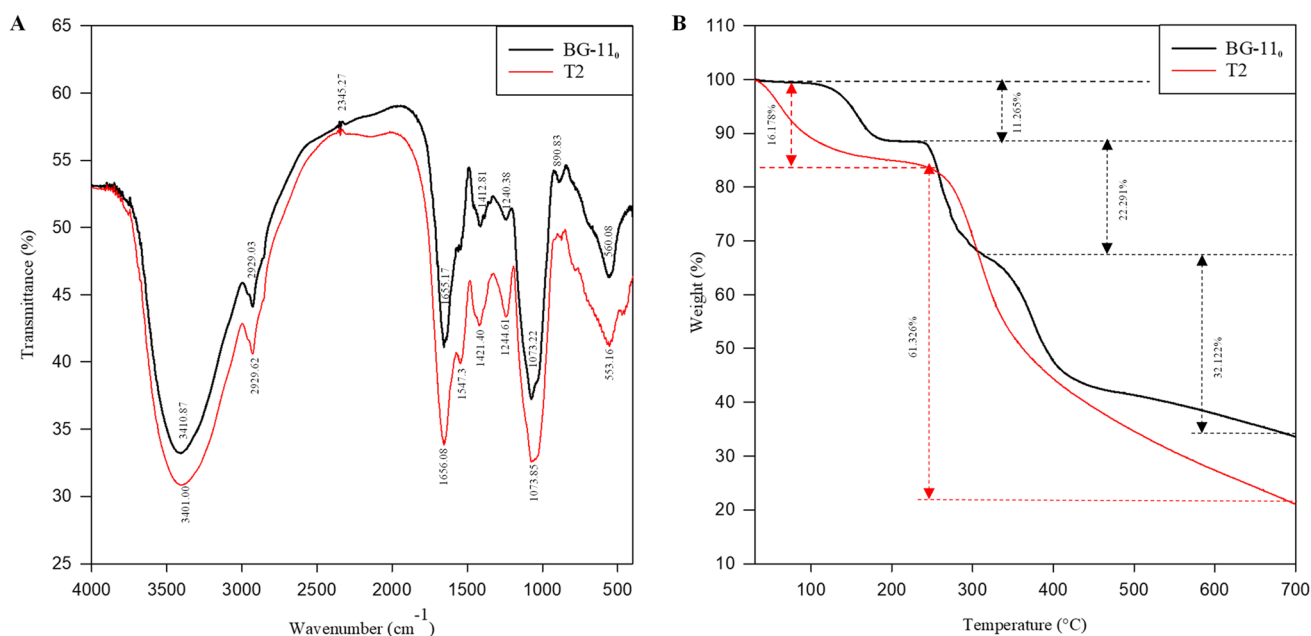


**Fig. 7** (A) FT-IR analysis and (B) thermogravimetric analysis of the exopolysaccharide of BG-11<sub>0</sub> and wastewater grown *Scytonema* sp. TPJ-3

Goyal 2005). The peak around 1655 cm<sup>-1</sup> was attributed to C=O stretch of carbonyl group. The presence of the protein molecules could be linked with the peak around 1547 cm<sup>-1</sup> under both BG11<sub>0</sub> and T2 conditions (Mihoubi et al. 2017). Stretching of COO – group detected at 1412 cm<sup>-1</sup> in BG-11<sub>0</sub> which was shifted to 1421.2 cm<sup>-1</sup> in T2 may be ascribed to the presence of uronic acids (De Philippis et al. 2011). The band attributed to sulfate ester O–S–O around 1240 cm<sup>-1</sup> and 1244 cm<sup>-1</sup> was found in BG-11<sub>0</sub> and T2 respectively, which suggested the sulfated nature of EPS (De Philippis et al. 2011). The band around 1073 cm<sup>-1</sup> in both conditions corresponded to the stretching vibration of C–O–C of glucose units (Yu and Irudayaraj 2005). The signal at 890 cm<sup>-1</sup> which corresponded to the β-glycosidic linkage was observed only in BG-11<sub>0</sub> (Alvarez et al. 2021) whereas peak at 560 cm<sup>-1</sup> in BG-11<sub>0</sub> and at 553 cm<sup>-1</sup> in T2 corresponded to the alkyl-halides (Kavita et al. 2014).

The FTIR spectra of EPS extracted from the BG-11<sub>0</sub> and wastewater condition (T2) did not show major changes. However, the presence of amide-II was observed only in wastewater condition which indicated that the EPS produced by TPJ-3 contains protein impurities. In order to confirm this, protein content in EPS was measured and the presence of 0.91% and 2.39% protein contents was found under BG-11<sub>0</sub> and T2 conditions respectively. The increased protein in exopolysaccharide might be due to secretion of extracellular enzymes, and proteins which may be involved in the degradation of contaminants or adhesion/cellular communication in response to pollutants

(López-Ortega et al. 2021) are present in wastewater. Moreover, this EPS-associated proteins may be enzymes that were possibly secreted by the cyanobacterium along with the EPS to degrade the utilizable substances present in the wastewater. In addition to these differences, the EPS consisted hydroxyl, carboxyl, carbonyl and amine groups which have the ability to chelate metal ions and such EPSs are also known for their antimicrobial properties (El Essawy et al. 2016). Furthermore, the uronic acid imparts negative charge and acidic property to the EPS which projects the metal-complexing capacity of EPS and this property is often used for the bioremediation purposes (De Philippis et al. 2011). Also, the sulfated EPSs have been reported for their unique physico-chemical (viscosifying and emulsifying) and biological properties (antimicrobial) (El Essawy et al. 2016). Therefore, the FTIR-based characterization of EPS produced by TPJ-3 confirmed its industrial suitability.

### Thermogravimetric analysis of EPS

The thermogram showing the TGA analysis of EPS extracted from BG-11<sub>0</sub> medium and T2 condition grown TPJ-3 is depicted in Fig. 7 B. The EPS from BG-11<sub>0</sub> was decomposed in three steps. In the first step, EPS lost 11.26% weight by elevating temperature from 30 to 240 °C, and thus, represented the elimination of moisture contents attached to carboxyl group as previously described (Kumar et al. 2004). The 22.29% weight loss was recorded in the second step which took place in the temperature range of

240 to 320 °C and corresponded to the removal of structural water conjugated with dehydration reaction. The third step that occurred in the temperature range of 320 to 700 °C showed 32.12% weight loss and involved depolymerization conjugated with the breakage of C–C and C–O bonds and leading to the formation of CO, CO<sub>2</sub> and H<sub>2</sub>O and decomposition of the remaining inorganic materials (Zamora et al. 2002).

The EPS from T2 grown TPJ-3 showed sequential degradation with an initial loss of 16.17% weight in the form of moisture content up to 250 °C. Subsequently, 61.32% weight was lost with elevation of temperature from 250 to 700 °C and attributed to dehydration, depolymerization and decomposition. Increasing temperature up to 700 °C resulted in the formation of graphitic carbon and poly nuclear aromatic structure, which was recorded about 34.32% and 22.49% under BG-11<sub>0</sub> and wastewater (T2) conditions respectively.

The TGA revealed the thermostability of the EPS obtained from both BG-11<sub>0</sub> and wastewater-grown culture was similar to that of *Cyanothece* sp., *Nostoc* sp. and *Oscillatoria* sp. (Parikh and Madamwar 2006). Therefore, it can be firmly said that the EPS of TPJ-3 could be a promising viscosifying, emulsifying, and biosorption agent at higher temperature also; however, further validation of this statement is still needed which requires higher level characterization of the EPS such as compositional and structural analyses via HPLC and NMR.

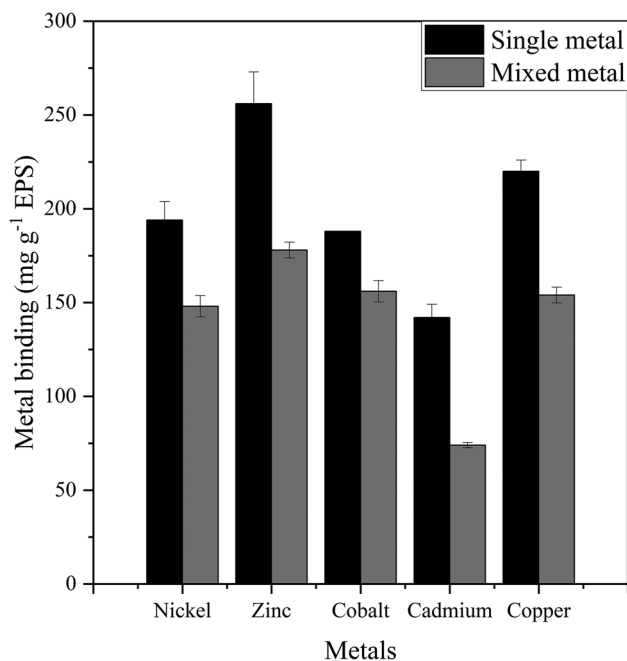


**Fig. 8** Metal-binding capacity of the exopolysaccharide produced by the strain *Scytonema* sp. TPJ-3

## Analysis of metal binding property of the EPS

The EPS extracted from the experimental cyanobacterium showed the highest affinity for the Zn in both the conditions (single and mixed) and the affinity to the cations followed the order Zn > Cu > Ni > Co > Cd (Fig. 8). As per our best knowledge, this is the first report of the metal binding capacity of the purified EPS extracted from the cyanobacteria which has excellent cation chelating potential as compared to bacterial EPS (Arias et al. 2003; Mata et al. 2008). The binding capacity of the EPS with the cations depends on the concentration of the charged components such as sulfate, phosphate, and uronic acids and the EPS of the isolated strain was already characterized which showed the presence of the abovementioned components through FTIR. The bio-compatible and eco-friendly ion-exchange resins can be developed using such EPS having great potential to chelate cations and can be used to remove potentially toxic element pollutants from the sewage, sludge, mines and other industries as an alternative to other physical and chemical methods which are not feasible to small industries and required high maintenance cost (De Philippis et al. 2011).

## Analysis of fatty acid methyl esters

The fatty acid profiling of BG-11<sub>0</sub>- and wastewater-grown culture showed that the fatty acid methyl esters (FAME) composition did not vary significantly (Table 3). The major fatty acids found in strain TPJ-3 were palmitic acid (C16:0), palmitoleic acid (C16:1), hexadecadienoic acid (C16:2), stearic acid (C18:0), oleic acid (C18:1), linoleic acid (C18:2), linolenic acid (C18:3) and stearidonic acid (C18:4). In both conditions, the palmitic acid (> 50%) and the stearic acid (> 2%) formed the major proportion of the total saturated fatty acids (> 60%), whereas the unsaturated fatty acid proportion was dominated by palmitoleic

**Table 3** Fatty acid profile of *Scytonema* sp. TPJ-3 grown in BG-11<sub>0</sub> and wastewater (T2)

Fatty acid (%)	BG-11 <sub>0</sub>	Wastewater (T2)
Palmitic acid C16:0	58.24	58.72
Palmitoleic acid C16:1	2.08	2.31
Hexadecadienoic acid C16:2	10.16	9.77
Stearic acid C18:0	2.59	2.19
Oleic acid C18:1	6.61	7.17
Linoleic acid C18:2	5.35	5.57
Linolenic acid C18:3	10.53	10.07
Stearidonic acid C18:4	4.43	4.23
Total saturated fatty acid	60.83	60.90
Total unsaturated fatty acid	39.17	39.10

acid (> 2%), hexadecadienoic acid (~10%), oleic acid (~7%), linoleic acid (> 5), linolenic acid (> 10%) and stearidonic acid (> 4%). In both conditions, the proportion of the total saturated and unsaturated fatty acids was about 61% and 39% respectively (Table 3). It was shown that the wastewater had neither positive nor negative impact on the FAME composition. The FAME of TPJ-3 comprised of short-chain fatty acids ( $C_{16}$ – $C_{18}$ ) with 69% of saturated and monounsaturated fatty acids which are most preferred fatty acids for the biodiesel production (Church et al. 2017), although the further evaluation of biodiesel properties of fatty acids in terms of kinematic viscosity, iodine value, cetane number and oxidative stability is required.

Besides, the fatty acids are primary metabolite; they are genetically determined and therefore conservative. The composition and relative percentage of individual fatty acids reflect the evolutionary changes in each genus or species along with biochemical processes in cyanobacteria. On the basis of differential composition of fatty acids, the cyanobacteria have been classified into four groups (Kenyon et al. 1972; Murata et al. 1992). The group I contains only saturated fatty acids; group II contains 16:1, 18:2 and 18:3 $\alpha$  but no 18:3 $\gamma$  or 18:4; group III contains 18:1, 18:2 and 18:3 $\gamma$  but neither 18:3 $\alpha$  nor 18:4; and group IV contains 18:1, 18:2, 18:3 $\alpha$ , 18:3 $\gamma$ , and 18:4. Therefore, according to the Kenyon-Murata classification system, the strain TPJ-3 corresponded to group IV. But it must be noticed that the very few numbers of investigated strains belonging to these genera hinder the clear taxonomic conclusions at the generic level. However, the chemotaxonomy of strain TPJ-3 will serve as a reference species for the future studies.

### Statistical analysis

The result obtained from statistical analysis (two-way ANOVA) exhibited that the changes in the means of different parameters were highly significant with the  $p$  value less than 0.001 ( $p < 0.001$ ) under different sets of time and conditions (Table S3). In order to understand the correlation between removal of pollutants and changes in cyanobacterial cellular constituents, with respect to different combinations of time and wastewater conditions, two separate PCA models were developed (Figs. 9 and 10) and the correlation among the corresponding components was presented in terms of their eigenvalues. From the scree plot of PCA1 pollutant removal model (Fig. 9), it was evident that the first two PCs were enough to explain 97.95% of the overall correlation. In PCA1 pollutant removal model, the major contributors of the PC1 were found to be salinity, conductivity, TDS, hardness, phosphate, sulfate, nitrate, nitrite, ammonium, chloride, Zn, Ni, Na, Ca and K, whereas the pH was identified as

the major contributor of PC2. As per PC1, both clusters 1 and 2 showed positive values but in respect to the PC2; cluster 1 showed positive value while cluster 2 reflected negative value. The high positive value of cluster 1 on the PC1 and PC2 axis indicated the high concentration of the pollutants in the wastewater on the initial day whereas the relatively lesser positive value of cluster 2 on PC1 and negative value on PC2 suggested very slight removal of the pollutants probably by the already-existing organisms in the naturally collected unautoclaved wastewater. Within the cluster 2, the higher negative value of day20/T1 as compared to day10/T1 on the PC2 axis enumerated small but time-dependent progressive removal of the pollutants. While the positive value of cluster 3 on the PC2 axis along with the high load of pH denoted enhancement of alkalinity, the high negative value of the same cluster with respect to PC1 pinpointed elevated removal of pollutants from the cyanobacterium inoculated autoclaved wastewater. Moreover, the higher negative value of day20/T2 as compared to day10/T2 of the cluster 3 on the PC1 axis suggested that the higher the incubation time the more the pollutant removal and alkalinity. In contrast to all other clusters, cluster 4 exhibited negative values on both PC1 and PC2 that indicated the maximum removal of the pollutants from the wastewater. This highest removal of the pollutants by the cyanobacterium in unautoclaved wastewater (T3) may be attributed to the functions of both the test cyanobacterium and other contaminating organisms. Again, the higher negative value of day20/T3 as compared to day10/T3 revealed the positive correlation between incubation time and removal of pollutants from the wastewater. Similarly, like the PCA1 scree plot, PCA2 cellular constituent model (Fig. 10) scree plot reflected that the first two PCs were sufficient to explain 97.72% of the overall correlation. In PCA2, the major contributors of the PC1 were observed to be biomass, chl *a*, protein, lipid, carbohydrate and EPS, whereas protein and lipid were identified as major contributors of the PC2. In PCA2, four different clusters (1 to 4) were obtained. Among these clusters, clusters 1 and 2 showed negative values on the PC1 whereas on the PC2, cluster 1 showed positive and cluster 2 showed negative values. The identical location of day0/BG-11<sub>0</sub>, day0/T2 and day0/T3 within cluster 1 was because of very initial day observations with similar contents of the variables. In contrast, slight enhancement of positivity on the PC2 of day10/T2, which was also a part of cluster 1, indicated the increased concentrations of the variables in the test cyanobacterium with increasing incubation time. The position of clusters 2 and 3 in the biplot revealed more positive correlation of day10/BG-11<sub>0</sub> and day20/BG-11<sub>0</sub> with only two variables, i.e., lipid and protein. The progressive increasing in positive value of day10/T3 and day20/T3 of cluster



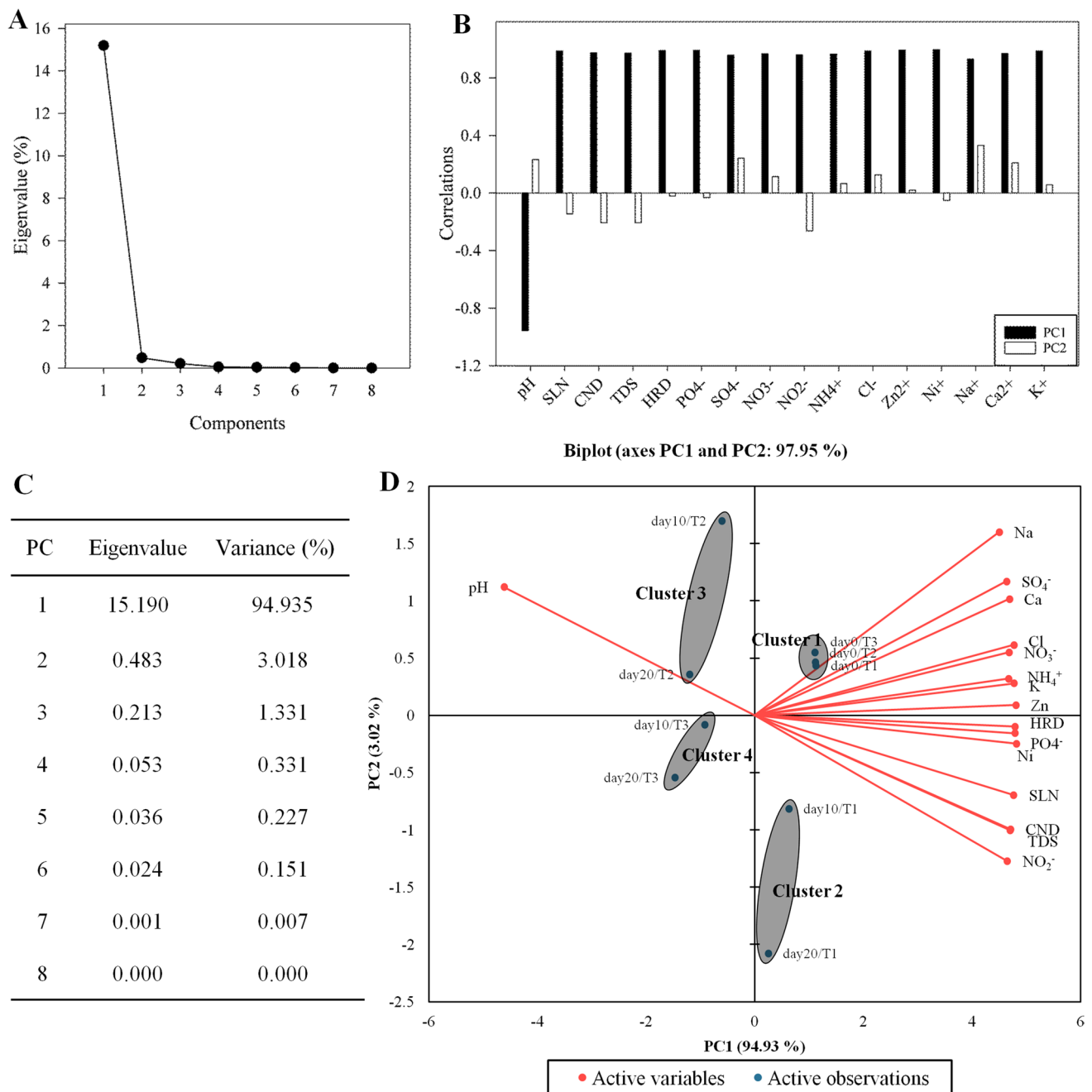


**Fig. 9** PCA1 pollutant removal model. **(A)** Scree plot, **(B)** loading of PC1 and PC2, **(C)** eigenvalue and variance (%) of PCs and **(D)** biplot of PCA1 pollutant removal model

3 on both PCs demonstrated the progressive increasing positive correlation with variables in order of carbohydrate > EPS > biomass > chl *a* respectively. In a nutshell, the PCA analysis firmly supported our experimental data. The PCA1 pollutant removal model and the PCA2 cellular constituent model reassured that the test cyanobacterium alone is highly efficient in removing pollutants from wastewater and producing high amount of carbohydrate, biomass, and EPS.

## Conclusion

The cyanobacterial strain TPJ-3 isolated from Tatapani hot spring is a novel species of the genus *Scytonema*. Since the Tatapani hot spring is located in Ambikapur district of the state Chhattisgarh, India, the cyanobacterium is named as *Scytonema ambikapurensis*. The cyanobacterium has considerable efficiency to bioremediate highly polluted

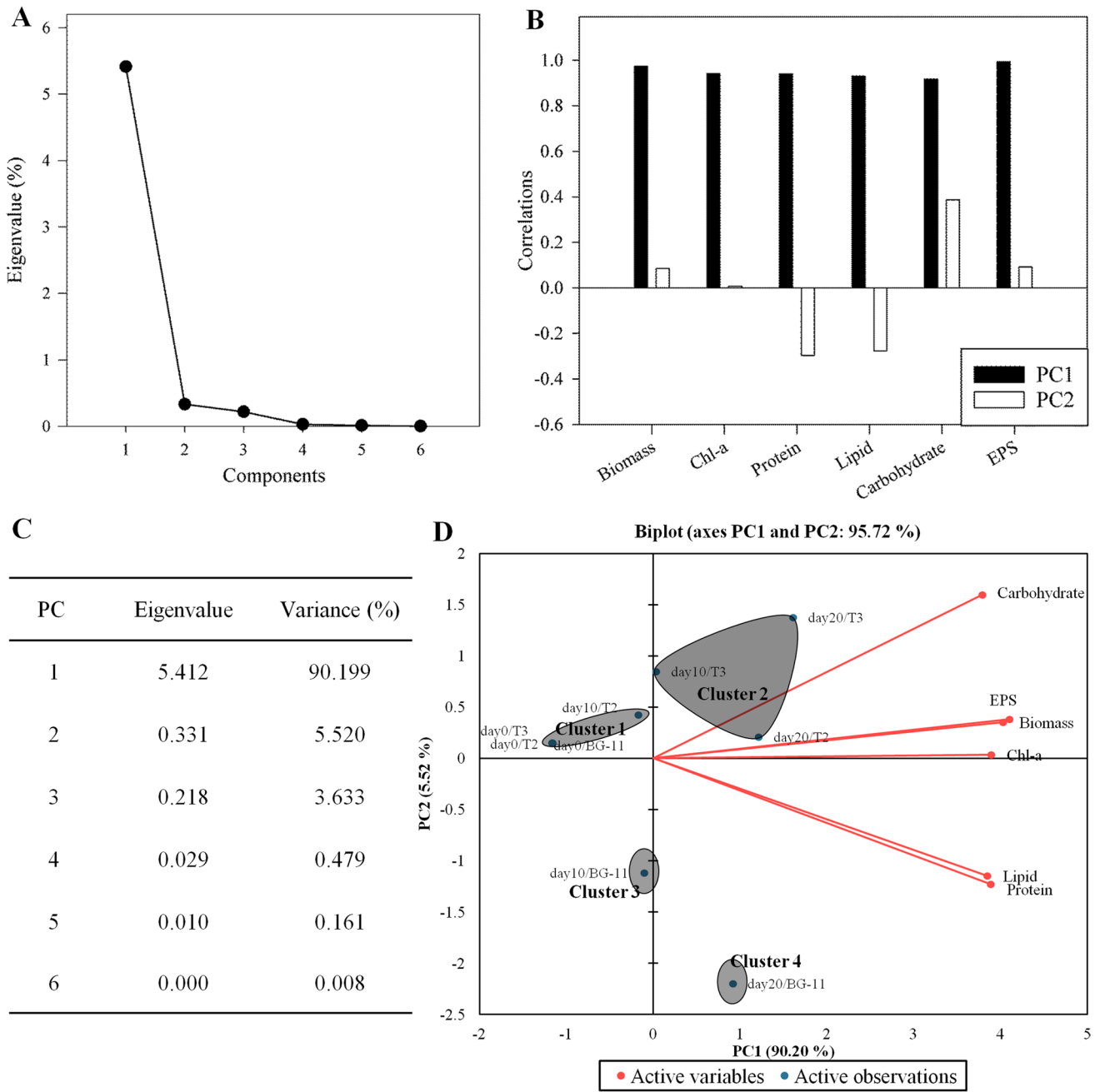


**Fig. 10** PCA2 cellular constituent model. (A) Scree plot, (B) loading of PC1 and PC2, (C) eigenvalue and variance (%) of PCs and (D) biplot of PCA2-cellular constituent model

wastewater (about complete removal of nitrogen sources, 86% phosphate, 81% Zn and 80% Ni) and simultaneously shows luxuriant growth with high production of biomass and EPS (up to 1.70-fold and 85% higher than the BG-11<sub>0</sub> respectively). While the bioremediation property of this organism reflected its environmental applicability, the production of high-temperature

stable EPS denoted its biotechnological and industrial values. Therefore, it can be concluded that the cyanobacterium is an outstanding bioagent to be used in wastewater treatment plants and at the same time, the cyanobacterium may also be used as a promising platform for the production of industrially valuable thermostable capsular EPS.

## Description of *Scytonema ambikapurensis* sp. nov.

**Etymology:** *Scytonema ambikapurensis* (am.bi.ka.pu.ren'sis. N.L. masc. adj. ambikapurensis, pertaining to district Ambikapur from where the strain was isolated).

**Description:** dark bluish green to brownish green, soft spongy, macroscopic mats found growing by adhere to the substratum on shallow water. The filaments are isopolar, uniseriate and densely entangled with solitary and geminate false branching. Sheath is prominent, thick, colorless and encloses the complete trichome. The vegetative cells are constricted, barrel shaped and usually wider than the length. The length of the vegetative cells is from 6.00 to 10.00  $\mu\text{m}$ , whereas the width is found to be 8.50–12.00  $\mu\text{m}$ . The terminal cells are distinctly marked and are yellowish in color with rounded end. The heterocytes are solitary as well as paired and are intercalary positioned. The ends of the heterocytes are both types concave as well as convex. The length of the heterocytes is ranges from 10.50 to 30.00  $\mu\text{m}$  and the width is ranges from 10.00 to 13.00  $\mu\text{m}$ . Akinetes not observed throughout the study.

**Type locality:** Tatapani hot spring, Ambikapur, Chhattisgarh, India (23.6986°N; 83.68404°E).

**Habitat:** Strain TPJ-3 was isolated from a hot spring field with temperature and pH of around 37 °C and 8.2 respectively. The habitat was characterized by 314  $\text{mg L}^{-1}$  salinity, 507  $\text{mg L}^{-1}$  total dissolved solid, 718  $\mu\text{S cm}^{-1}$  conductivity and 95  $\text{mg L}^{-1}$  alkalinity. The sulfate concentration was found to be 89  $\text{mg L}^{-1}$ . The ionic concentration and dominance was found to be  $\text{Na}^+$  (812  $\text{mg L}^{-1}$ ) >  $\text{K}^+$  (23  $\text{mg L}^{-1}$ ) >  $\text{Ca}^{++}$  >  $\text{Ni}^{++}$  >  $\text{Mg}^{++}$  (< 0.5  $\text{mg L}^{-1}$ ).

**Holotype (here designated):** portion of a culture of *Scytonema ambikapurensis* is preserved in metabolically inactive form in National Agriculturally Important Microbial Culture Collection (NAIMCC) and available under the accession number NAIMCC-CC-00358.

**Supplementary Information** The online version contains supplementary material available at <https://doi.org/10.1007/s11356-023-26032-2>.

**Acknowledgements** We are thankful to the Head, Department of Botany, Banaras Hindu University, Varanasi, India, for providing laboratory facilities; Central Instrumentation Facility, Department of Botany, Banaras Hindu University; Interdisciplinary School of Life Sciences (ISLS), Banaras Hindu University, for confocal microscopy; Central instrumental facility, Department of Chemistry, Banaras Hindu University, for FTIR and TGA facility; Advanced Instrumentation Research Facility (AIRF), Jawaharlal Nehru University, Delhi, for GC-MS facility. We are thankful to Professor Kalluri V. S. Rangnath, Department of Chemistry, Banaras Hindu University, for valuable suggestions.

**Author contribution** Material preparation, data collection, data analysis and writing original draft were performed by Tameshwar Prasad Jaiswal and Sindhunath Chakraborty; the first draft of the manuscript was written by Sanjay Sharma and Aditi Mishra. Validation,

supervision and final editing were performed by Arun Kumar Mishra and Satya Shila Singh. All authors read and approved the final manuscript. Tameshwar Prasad Jaiswal and Sindhunath Chakraborty contributed equally.

**Funding** Tameshwar Prasad Jaiswal is also thankful to University Grant Commission, Delhi, for awarding Senior Research Fellowship. Satya Shila Singh is also thankful to Institute of Eminence (IOE-6031), Banaras Hindu University, for the financial support. The authors are also thankful to the Indian Council of Agricultural Research–Application of Microorganisms in Agriculture and Allied Sector (ICAR-AMAAS) for the financial support.

**Data availability** The datasets and materials used during the current study are available from the corresponding author on reasonable request.

## Declarations

**Ethical approval and consent to participate** Not applicable

**Consent for publication** Not applicable

**Conflict of interest** The authors declare no competing interests.

## References

- Ahluwalia SS, Goyal D (2005) Removal of heavy metals by waste tea leaves from aqueous solution. *Eng Life Sci* 5:158–162. <https://doi.org/10.1002/elsc.200420066>
- Aketo T, Hoshikawa Y, Nojima D, Yabu Y, Maeda Y, Yoshino T, Takano H, Tanaka T (2020) Selection and characterization of microalgae with potential for nutrient removal from municipal wastewater and simultaneous lipid production. *J Biosci Bioeng* 129:565–572. <https://doi.org/10.1016/j.jbiosc.2019.12.004>
- Alvarez X, Alves A, Ribeiro MP, Lazzari M, Coutinho P, Otero A (2021) Biochemical characterization of *Nostoc* sp. exopolysaccharides and evaluation of potential use in wound healing. *Carbohydr Polym* 254. <https://doi.org/10.1016/j.carbpol.2020.117303>
- APHA (2005) Standard methods for the examination of water and wastewater. American Public Health Association, Washington DC
- Arias DM, Uggetti E, García J (2020a) Assessing the potential of soil cyanobacteria for simultaneous wastewater treatment and carbohydrate-enriched biomass production. *Algal Res* 51:102042. <https://doi.org/10.1016/j.algal.2020.102042>
- Arias DM, Uggetti E, García J (2020b) Assessing the potential of soil cyanobacteria for simultaneous wastewater treatment and carbohydrate-enriched biomass production. *Algal Res* 51:102042. <https://doi.org/10.1016/j.algal.2020.102042>
- Arias S, Del Moral A, Ferrer MR, Tallon R, Quesada E, Béjar V (2003) Mauran, an exopolysaccharide produced by the halophilic bacterium *Halomonas maura*, with a novel composition and interesting properties for biotechnology. *Extremophiles* 7:319–326. <https://doi.org/10.1007/s00792-003-0325-8>
- Banerjee A, Sarkar S, Govil T, González-Faune P, Cabrera-Barjas G, Bandopadhyay R, Salem DR, Sani RK (2021) Extremophilic exopolysaccharides: biotechnologies and wastewater remediation. *Front Microbiol* 12. <https://doi.org/10.3389/fmicb.2021.721365>
- Bohutskiy P, Kligerman DC, Byers N et al (2016) Effects of inoculum size, light intensity, and dose of anaerobic digestion centrate on growth and productivity of *Chlorella* and *Scenedesmus* microalgae

- and their poly-culture in primary and secondary wastewater. *Algal Res* 19:278–290. <https://doi.org/10.1016/j.algal.2016.09.010>
- Bradford MM (1976) A rapid and sensitive method for the quantitation of microgram quantities of protein utilizing the principle of protein-dye binding. *Anal Biochem* 72:248–254. [https://doi.org/10.1016/0003-2697\(76\)90527-3](https://doi.org/10.1016/0003-2697(76)90527-3)
- Cataldo DA, Maroon M, Schrader LE, Youngs VL (1975) Communications in soil science and plant analysis rapid colorimetric determination of nitrate in plant tissue by nitration of salicylic acid. *Commun Soil Sci Plant Anal* 37–41. <https://doi.org/10.1080/00103627509366547>
- Cepoi L, Rudi L, Chiriac T, Codreanu S, Valuța A (2016) Biological methods of wastewater treatment. In: Zinicovscaia I, Cepoi L. (eds) *Cyanobacteria for bioremediation of wastewaters*. Springer, Cham, Pp 45–60 [https://doi.org/10.1007/978-3-319-26751-7\\_5](https://doi.org/10.1007/978-3-319-26751-7_5)
- Chakraborty S, Mishra AK (2020) Mitigation of zinc toxicity through differential strategies in two species of the cyanobacterium *Anabaena* isolated from zinc polluted paddy field. *Environ Pollut* 263:114375. <https://doi.org/10.1016/j.envpol.2020.114375>
- Chevalier P, Proulx D, Lessard P, Vincent WF, De la Noüe J (2000) Nitrogen and phosphorus removal by high latitude mat-forming cyanobacteria for potential use in tertiary wastewater treatment. *J Appl Phycol* 12:105–112. <https://doi.org/10.1023/A:1008168128654>
- Church J, Hwang JH, Kim KT, McLean R, Oh YK, Nam B, Joo JC, Lee WH (2017) Effect of salt type and concentration on the growth and lipid content of *Chlorella vulgaris* in synthetic saline wastewater for biofuel production. *Bioresour Technol* 243:147–153. <https://doi.org/10.1016/j.biortech.2017.06.081>
- Crini G, Lichtfouse E (2019) Advantages and disadvantages of techniques used for wastewater treatment. *Environ Chem Lett* 17:145–155. <https://doi.org/10.1007/s10311-018-0785-9>
- De Philippis R, Colica G, Micheletti E (2011) Exopolysaccharide-producing cyanobacteria in heavy metal removal from water: molecular basis and practical applicability of the biosorption process. *Appl Microbiol Biotechnol* 92:697–708. <https://doi.org/10.1007/s00253-011-3601-z>
- Desikachary TV (1959) *Cyanophyta*. Indian Council of Agricultural Research, New Delhi
- Dubois M, Gilles K, Hamilton JK, Rebers PA, Smith F (1951) A colorimetric method for the determination of sugars. *Nature* 168:167. <https://doi.org/10.1038/168167a0>
- Edwards U, Rogall T, Blöcker H, Emde M, Böttger EC (1989) Isolation and direct complete nucleotide determination of entire genes. *Nucleic Acids Res* 17:7843–7853
- El Essawy AK, Abu Shady HM, Abu El Kher AM, Helal MM (2016) Antimicrobial, anticoagulation, fibrinolytic and prebiotic activities of exopolysaccharide produced by marine *Klebsiella* Sp. *Egypt J Exp Biol (Bot)* 12(2):267–274. <https://doi.org/10.5455/egyjobb.20161115114843>. ISSN: 2090 – 0503
- Geddie JL, Sutherland IW (1993) Uptake of metals by bacterial polysaccharides. *J Appl Bacteriol* 74:467–472. <https://doi.org/10.1111/j.1365-2672.1993.tb05155.x>
- Gkelis S, Rajaniemi P, Vardaka E et al (2005) *Limnothrix redekei* (Van Goor) Meffert (Cyanobacteria) strains from Lake Kastoria, Greece form a separate phylogenetic group. *Microb Ecol* 49:176–182. <https://doi.org/10.1007/s00248-003-2030-7>
- Huertas MJ, López-Maury L, Giner-Lamia J, Sánchez-Riego AM, Florêncio FJ (2014) Metals in cyanobacteria: analysis of the copper, nickel, cobalt and arsenic homeostasis mechanisms. *Life* 4:865–886. <https://doi.org/10.3390/life4040865>
- Jaiswal TP, Chakraborty S, Singh P, Mishra AK, Singh SS (2021) Description of hot spring dwelling *Mastigocladus ambikapurensis* sp. nov., using a polyphasic approach. *Plant Syst Evol* 307:1–12. <https://doi.org/10.1007/s00606-021-01755-2>
- Janczarek M, Rachwał K, Cieślą J, Ginalska G, Bieganski A (2015) Production of exopolysaccharide by *Rhizobium leguminosarum* *bv. trifolii* and its role in bacterial attachment and surface properties. *Plant Soil* 388:211–227. <https://doi.org/10.1007/s11104-014-2320-5>
- Kalpna R, Angelaalincy MJ, Kamatchirajan BV, Vasantha VS, Ashokkumar B, Ganesh V, Varalakshmi P (2018) Exopolysaccharide from *Bacillus cereus* VK1: enhancement, characterization and its potential application in heavy metal removal. *Colloids Surfaces B Biointerfaces* 171:327–334. <https://doi.org/10.1016/j.colsurfb.2018.07.043>
- Kang JX, Wang J (2005) A simplified method for analysis of polyunsaturated fatty acids. *BMC Biochem* 6:4–7. <https://doi.org/10.1186/1471-2091-6-5>
- Kavita K, Singh VK, Mishra A, Jha B (2014) Characterisation and anti-biofilm activity of extracellular polymeric substances from *Oceanobacillus theyensis*. *Carbohydr Polym* 101:29–35. <https://doi.org/10.1016/J.CARBPOL.2013.08.099>
- Kenyon CN, Rippka R, Stanier RY (1972) Fatty acid composition and physiological properties of some filamentous blue-green algae. *Arch Mikrobiol* 83:216–236. <https://doi.org/10.1007/BF00645123>
- Khattar JIS, Singh DP, Jindal N, Kaur N, Singh Y, Rahi P, Gulati A (2010) Isolation and characterization of exopolysaccharides produced by the cyanobacterium *Limnothrix redekei* PUPCCC 116. *Appl Biochem Biotechnol* 162:1327–1338. <https://doi.org/10.1007/s12010-010-8922-3>
- Kishi M, Yamada Y, Katayama T, Matsuyama T, Toda T (2020) Carbon mass balance in *Arthrospira platensis* culture with medium recycle and high CO<sub>2</sub> supply. *Appl Sci* 10. <https://doi.org/10.3390/app10010228>
- Komárek J. (2013) Süßwasserflora von Mitteleuropa, Bd. 19/3: Cyanoprocaryota. Süßwasserflora von Mitteleuropa, Bd. 19/3 Cyanoprocaryota. <https://doi.org/10.1007/978-3-8274-2737-3>
- Kumar CG, Joo HS, Choi JW, Koo YM, Chang CS (2004) Purification and characterization of an extracellular polysaccharide from haloalkalophilic *Bacillus* sp. I-450. *Enzyme Microb Technol* 34:673–681. <https://doi.org/10.1016/j.enzmictec.2004.03.001>
- Li P, Harding SE, Liu Z (2001) Cyanobacterial exopolysaccharides: their nature and potential biotechnological applications. *Biotechnol Genet Eng Rev* 18:375–404. <https://doi.org/10.1080/02648725.2001.10648020>
- López-Ortega MA, Chavarría-Hernández N, López-Cuellar M del R, Rodríguez-Hernández AI (2021) A review of extracellular polysaccharides from extreme niches: an emerging natural source for the biotechnology From the adverse to diverse! *Int J Biol Macromol* 177:559–577. <https://doi.org/10.1016/j.ijbiomac.2021.02.101>
- Mata JA, Béjar V, Bressollier P, Tallon R, Urdaci MC, Quesada E, Llamas I (2008) Characterization of exopolysaccharides produced by three moderately halophilic bacteria belonging to the family Alteromonadaceae. *J Appl Microbiol* 105:521–528. <https://doi.org/10.1111/j.1365-2672.2008.03789.x>
- Mihoubi W, Sahli E, Gargouri A, Amiel C (2017) FTIR spectroscopy of whole cells for the monitoring of yeast apoptosis mediated by p53 over-expression and its suppression by *Nigella sativa* extracts. *PLoS One* 12(7):e0180680. <https://doi.org/10.1371/journal.pone.0180680>
- Mishra D, Saraf A, Kumar N, Pal S, Singh P (2021) Issues in cyanobacterial taxonomy: Comprehensive case study of unbranched, false branched and true branched heterocytous cyanobacteria. *FEMS Microbiol Lett* 368:1–10. <https://doi.org/10.1093/femsle/fnab005>
- Morillo JA, Aguilera M, Ramos-Cormenzana A, Monteoliva-Sánchez M (2006) Production of a metal-binding exopolysaccharide by *Paenibacillus jamilae* using two-phase olive-mill waste as fermentation substrate. *Curr Microbiol* 53:189–193. <https://doi.org/10.1007/s00284-005-0438-7>
- Mukherjee C, Mukherjee C, Ray K (2015) An improved DAPI staining procedure for visualization of polyphosphate granules in cyanobacterial



- and microalgal cells. *Protoc Exch* 6–9. <https://doi.org/10.1038/protex.2015.066>
- Murata N, Wada H, Gombos Z (1992) Modes of fatty-acid desaturation in cyanobacteria. *Plant Cell Physiol* 33:933–941. <https://doi.org/10.1093/oxfordjournals.pcp.a078344>
- Parihk A, Madamwar D (2006) Partial characterization of extracellular polysaccharides from cyanobacteria. *Bioresour Technol* 97:1822–1827. <https://doi.org/10.1016/j.biortech.2005.09.008>
- Pereira S, Micheletti E, Zille A, Santos A, Ferreira PM, Tamagnini P, De Philippis R (2011) Using extracellular polymeric substances (EPS)-producing cyanobacteria for the bioremediation of heavy metals: do cations compete for the EPS functional groups and also accumulate inside the cell? *Microbiology* 157:451–458. <https://doi.org/10.1099/mic.0.041038-0>
- Ramesh ST, Rameshbabu N, Gandhimathi R, Nidheesh PV, Kumar MS (2012) Kinetics and equilibrium studies for the removal of heavy metals in both single and binary systems using hydroxyapatite. *Appl Water Sci* 2:187–197. <https://doi.org/10.1007/s13201-012-0036-3>
- Rippka R, Deruelles J, Waterbury JB (1979) Generic assignments, strain histories and properties of pure cultures of cyanobacteria. *J Gen Microbiol* 111:1–61. <https://doi.org/10.1099/00221287-111-1-1>
- Ritchie RJ (2006) Consistent sets of spectrophotometric chlorophyll equations for acetone, methanol and ethanol solvents. *Photosynth Res* 89:27–41. <https://doi.org/10.1007/s11120-006-9065-9>
- Samiotis G, Stamatakis K, Amanatidou E (2021) Assessment of *Synechococcus elongatus* PCC 7942 as an option for sustainable wastewater treatment. *Water Sci Technol* 84(6):1438–1451. <https://doi.org/10.2166/wst.2021.319>
- Samiotis G, Ziagova MG, Amanatidou E (2022) Wastewater substrate disinfection for cyanobacteria cultivation as tertiary treatment. *Environ Sci Pollut Res*. <https://doi.org/10.1007/s11356-022-20369-w>
- Sanz-Luque E, Bhaya D, Grossman AR (2020) Polyphosphate: a multifunctional metabolite in cyanobacteria and algae. *Front Plant Sci* 11:1–21. <https://doi.org/10.3389/fpls.2020.00938>
- Saraf A, Dawda HG, Suradkar A, Batule P, Behere I, Kotulkar M, Kumat A, Singh P (2018) Insights into the phylogeny of false-branching heterocytous cyanobacteria with the description of *Scytonema pachmarhiense* sp. Nov. isolated from Pachmarhi Biosphere Reserve. *India FEMS Microbiol Lett* 365:1–9. <https://doi.org/10.1093/femsle/fny160>
- Shahid A, Malik S, Zhu H, Xu J, Nwaz MZ, Nwaz S, Alam MA, Mehmood MA (2020) Cultivating microalgae in wastewater for biomass production, pollutant removal, and atmospheric carbon mitigation; a review. *Sci Total Environ* 704:135303. <https://doi.org/10.1016/j.scitotenv.2019.135303>
- Singh AL (2011) Study of physico-chemical characteristics of water samples from Assi river, Varanasi, U.P. India *Pollut Res* 30:209–212
- Singh DP, Khattar JS, Rajput A, Chaudhary R, Singh R (2019) High production of carotenoids by the green microalga *Asterarcys quadricellulare* PUMCC 5.1.1 under optimized culture conditions. *PLoS One* 14. <https://doi.org/10.1371/journal.pone.0221930>
- Sutherland DL, Ralph PJ (2019) Microalgal bioremediation of emerging contaminants - opportunities and challenges. *Water Res* 164:114921. <https://doi.org/10.1016/j.watres.2019.114921>
- Tamura K, Peterson D, Peterson N, Stecher G, Nei M, Kumar S (2011) MEGA5: molecular evolutionary genetics analysis using maximum likelihood, evolutionary distance, and maximum parsimony methods. *Mol Biol Evol* 28:2731–2739. <https://doi.org/10.1093/molbev/msr121>
- Whitton R, Le Mével A, Pidou M, Ometto F, Villa R, Jefferson B (2016) Influence of microalgal N and P composition on wastewater nutrient remediation. *Water Res* 91:371–378. <https://doi.org/10.1016/j.watres.2015.12.054>
- Wu L, Zhu Q, Yang L, Li B, Hu C, Lan S (2018) Nutrient transferring from wastewater to desert through artificial cultivation of desert cyanobacteria. *Bioresour Technol* 247:947–953. <https://doi.org/10.1016/j.biortech.2017.09.127>
- Yu C, Irudayaraj J (2005) Spectroscopic characterization of microorganisms by Fourier transform infrared microspectroscopy. *Biopolymers* 77:368–377. <https://doi.org/10.1002/bip.20247>
- Yi YC, Jean Z (2011) Rapid quantitative analysis of lipids using a colorimetric method in a microplate format. *Lipids* 95–103. <https://doi.org/10.1007/s11745-010-3494-0>
- Zamora F, González MC, Dueñas MT, Irastorza A, Velasco S, Ibarburu I (2002) Thermodegradation and thermal transitions of an exopolysaccharide produced by *Pediococcus damnosus* 2.6. *J Macromol Sci - Phys* 41 B:473–486. <https://doi.org/10.1081/MB-120004348>
- Zhu Q, Wu L, Li G, Li X, Zhao C, Du C, Wang F, Li W, Zhang L (2021) A novel of transforming wastewater pollution into resources for desertification control by sand-consolidating cyanobacteria, *Scytonema javanicum*. *Environ Sci Pollut Res* 28:13861–13872. <https://doi.org/10.1007/s11356-020-11553-x>
- Zuker M (2003) Mfold web server for nucleic acid folding and hybridization prediction. *Nucleic Acids Res* 31:3406–3415. <https://doi.org/10.1093/nar/gkg595>

**Publisher's note** Springer Nature remains neutral with regard to jurisdictional claims in published maps and institutional affiliations.

Springer Nature or its licensor (e.g. a society or other partner) holds exclusive rights to this article under a publishing agreement with the author(s) or other rightsholder(s); author self-archiving of the accepted manuscript version of this article is solely governed by the terms of such publishing agreement and applicable law.